

**REVIEW** OPEN ACCESS

# Packaging of Macroscopic Material Payloads: Needs, Challenges, Concepts, and Future Directions

 Venkata S. R. Jampani<sup>1</sup>  | Manos Anyfantakis<sup>2</sup> 
<sup>1</sup>Condensed Matter Physics Department, Jožef Stefan Institute, Ljubljana, Slovenia | <sup>2</sup>European Space Resources Innovation Centre, Luxembourg Institute of Science and Technology, Esch-sur-Alzette, Luxembourg

**Correspondence:** Venkata S. R. Jampani ([vsrao.jampani@ijs.si](mailto:vsrao.jampani@ijs.si)) | Manos Anyfantakis ([emmanouil.anyfantakis@list.lu](mailto:emmanouil.anyfantakis@list.lu))

**Received:** 9 September 2025 | **Revised:** 30 January 2026 | **Accepted:** 2 February 2026

**Keywords:** encapsulation | interface science | macroscopic payloads | packaging | responsive/smart packaging

## ABSTRACT

The packaging of various material goods is a necessary element in numerous sectors, ranging from the food and pharmaceutical industry to biotechnology and medicine to space missions. Packaging has a multifaceted complexity inherently linked to both the properties of the materials involved and the requirements of the intended application. This level of complexity calls for the development of smart materials engineering solutions, necessitating crossing the boundaries between various science disciplines. Despite this, discussions of packaging often remain fragmented by industrial sector and rarely treat it as a materials science and interfacial engineering problem. Here, we introduce a unified framework that decomposes any packaging system into the payload, packaging material, and packaging strategy, and combines them into a conceptual packaging equation: packaging strategy = payload + packaging material. We focus on payloads with sizes (volumes) ranging from approximately 100  $\mu\text{m}$  ( $\sim\text{pL}$ ) to 1 cm ( $\sim\text{mL}$ ) and review relevant packaging strategies developed. To offer a systematic analysis, we categorize packaging strategies by the phase of the payload, and provide illustrative examples involving liquids, gases, solids, and mixed-phase payloads. Moreover, we discuss strategies based on their functionality (neutral, multifunctional, responsive) and packaging application location (in situ vs. ex situ). Our analysis is largely from the perspective of soft matter and interface science. Besides forming the basis of many of the examples discussed, these fields offer exciting opportunities for future research on packaging, both from a materials standpoint and a conceptual perspective. This includes the development necessary for smart packaging strategies that combine multifunctionality with responsiveness, as well as addressing traditional (e.g., cost-efficiency, scaling up) and emerging (e.g., sustainability, end-of-life) challenges. We intend to stimulate creativity and encourage interdisciplinary collaboration by inviting researchers and engineers from diverse fields to contribute novel ideas for addressing a truly complex yet highly fascinating problem.

## 1 | Introduction

### 1.1 | Packaging of Various Materials Across Diverse Scales and Industries: Familiar Examples

Most material goods are not consumed where they are produced; instead, they require packaging for handling, transportation, and storage under diverse mechanical, chemical, and regulatory constraints [1]. Let us consider milk as an example of a food product in liquid form: It is collected directly from animals at the source

and undergoes packaging for transportation to processing plants in large containers (volume on the order of  $\sim\text{m}^3$ ) and subsequently smaller consumer-friendly sizes ( $\sim 1\text{ L}$ , Figure 1i) [3–5]. At smaller volume scales, around a few milliliters, creamers of condensed milk wrapped in aluminum packages are used [6]. Gelatin capsules containing supplements like omega-3 oil (Figure 1ii) are another everyday example from the food industry, based on liquid packaging at even smaller volumes, on the order of microliters. Pharmaceuticals also rely on packaging,

This is an open access article under the terms of the [Creative Commons Attribution-NonCommercial-NoDerivs](https://creativecommons.org/licenses/by-nc-nd/4.0/) License, which permits use and distribution in any medium, provided the original work is properly cited, the use is non-commercial and no modifications or adaptations are made.

© 2026 The Author(s). *Advanced Engineering Materials* published by Wiley-VCH GmbH.

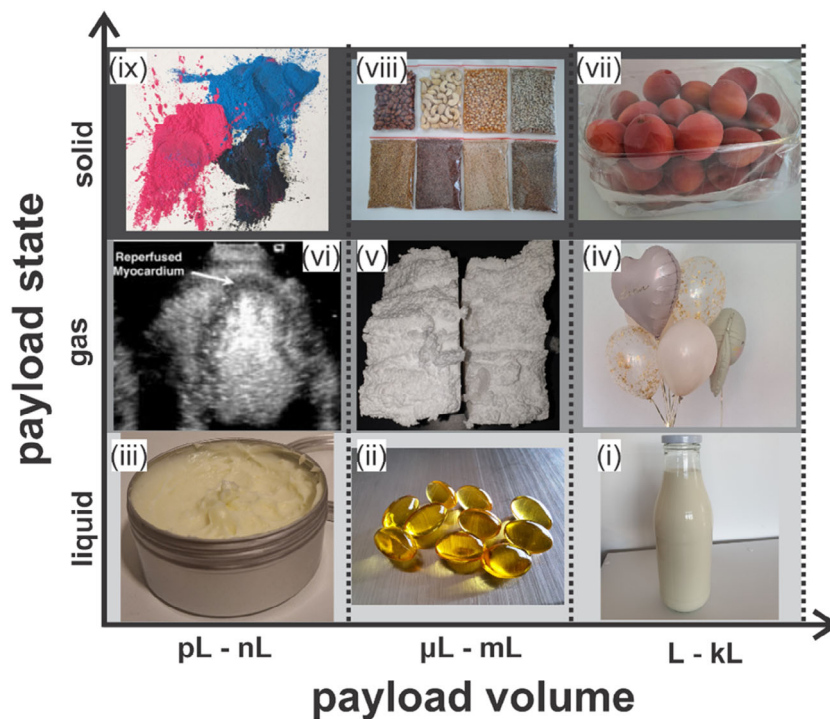


**FIGURE 1** | The diversity and complexity of packaging are illustrated by familiar examples of packaging liquids (i–iii), gases (iv–vi), and solids (vii–ix). (i) Milk packaged in a glass bottle sealed with a metal cap. (ii) Gelatin capsules containing omega-3 fatty acids. (iii) A cosmetic cream based on liposomes, used for packaging active ingredients at the nanoscale. (iv) Balloons comprising He packaged by a metal-coated poly(ethylene terephthalate) film. (v) Extruded poly(styrene) foam features uniform cells containing air. (vi) Gas-filled microbubbles packaged with nanomaterials (lipids, proteins, polymers) enhance the contrast in ultrasound imaging; see image of the left ventricle of a healthy heart, reproduced with permission [2]. Copyright 2003, Wiley. (vii) Fruits as a representative example of packaged macroscopic solids in the food industry; the packaging materials are often poly(propylene) and low-density poly(ethylene), for the basket and wrapping foil, respectively. (viii) Spices are packaged in small volumes using polymer bags (typically poly(ethylene terephthalate) or high-density poly(ethylene)). (ix) Toners comprise pigments enclosed within polymer microparticles.

specifically of active substances, across multiple volume scales. Systems for oral drug administration, such as gelatin capsules containing ibuprofen, are about several microliters in volume [7]. Nanocapsules further reduce the characteristic volume scale, enclosing active ingredients in volumes as tiny as 50 femtoliters [8, 9]. Although we cannot see packages in the nanoscale, we are familiar with products containing them, such as liposome-based cosmetic creams (Figure 1iii).

Gaseous payloads typically require robust containment because of the increased mobility of molecules in the gas phase, often combined with the high pressure used for storage. Packaging large gas volumes (~kL and beyond) securely is vital for safe transport and utilization across various industries, including food packaging, healthcare, and space missions, where leakage control and maintaining purity are paramount. More familiar examples range from helium-filled balloons (typically ~L) used for decoration (Figure 1iv) to air-filled soap bubbles (typically mL-L) used for entertainment, sparking the interest of kids and curious adults alike [10]. The construction industry uses packaged air for insulation purposes, a familiar example being extruded poly(styrene) foam (~hundreds of  $\mu\text{m}$ , ~pL, Figure 1v). Some medical procedures rely on microscopic gas packages; for instance, microbubbles containing, e.g., air, nitrogen, or perfluorocarbons (~fL), are employed in ultrasound imaging (Figure 1vi) [2, 11].

Numerous industries are directly concerned with the packaging of solid goods. The construction industry handles material

volumes of thousands of cubic meters, whereas the pharmaceutical sector utilizes precise encapsulation of active ingredients ranging from milliliters to microliters and even picoliters [12, 13]. The food industry also extensively packs solid products, with solutions available for various volumes, from large poly(ethylene) containers (~dL to kL) for bulk to smaller individual wrappers (~L to tens of mL) [14]. Examples of packaging solid food products include fruits (Figure 1vii) and vegetables (~L), or more expensive ingredients like spices (Figure 1, viii) and food additives (~ $\mu\text{L}$  to mL) [15]. Besides food, other commonly used products rely on packaging solid materials at the microscale, such as toners used in laser printers that often comprise polymer microbeads (~pL) enclosing pigments and additives (Figure 1ix).

Clearly, packaging is a key prerequisite for the numerous applications developed by the diverse industries mentioned above, and many others, such as cosmetics, biotechnology, and nanotechnology [1, 13, 14, 16–21]. Essentially, the nature of a given application dictates the requirements of the packaging strategy. A key requirement is that packaging accommodates the volume of material to be contained, which, as illustrated above, may span an impressive breadth, from at least megaliters down to femtoliters [22]. Other common requirements are that the packaging material primarily preserves the sample and prolongs its life without interfering with the physical and chemical characteristics of the packaged products. Additionally, it is often desirable that the packaging material is biodegradable, acts as an  $\text{O}_2$  scavenger, inhibits volatile gases

and radiation, controls the permeation of water vapor, controls drug release, and has antimicrobial properties [9, 21, 23]. Generally, it is also advantageous to have transparent packaging material that allows visual inspection of the content [24, 25]. More elaborate requirements arise from advanced applications; for instance, the packaging material may also serve as a sensor to monitor the quality of the packaged products and showcase their status to consumers in a readily accessible manner [26]. Before developing a desired packaging solution, these requirements must be thoroughly analyzed and well understood.

## 1.2 | Key Concepts and Terminology Used in This Article

The extensive scope of packaging research has motivated scientists and engineers from various disciplines to develop various packaging strategies. This has led to a wide range of concepts and terms being used, which can be difficult for both newcomers and experienced researchers to navigate. To describe examples of packaging concepts from various disciplines within a unified and straightforward framework, we introduce below the basic terminology used throughout this article. For each term used here, we also list various terms used by other authors, which we consider identical or similar in content. Our purpose is to present a pedagogical approach to discussing various packaging strategies described in the literature.

### 1.2.1 | Payload

*Definition:* Any material intended to be packaged, irrespective of its physical state (solid, liquid, gas, or any combination of these) or volume/mass (microscopic to macroscopic range).

*Synonyms:* Terms such as “cargo,” “core material,” “encapsulated material,” and “encapsulate” have been commonly used in the literature [26].

*Characteristics:* Payloads may include pharmaceutical ingredients (molecular scale), living cells (microscopic scale), or products like beverages and fresh produce (macroscopic scale) [13, 27–29].

### 1.2.2 | Packaging Material

*Definition:* A material of any physical form (solid, fluid, or combination of these) used to contain or protect the payload from external conditions.

*Synonyms:* Alternative terms are “encapsulant,” “wrapper,” “shell,” or “membrane”, [30].

*Characteristics:* Packaging materials may consist of building blocks with various characteristic length scales. At the molecular scale, surfactants are used to package air, yielding soap bubbles. To increase longevity or size, polymers like guar gum are introduced, forming multiscale packaging materials comprising both molecular and macromolecular building blocks [10]. Packaging materials comprising other mesoscopic building blocks are exemplified by liquid marbles, where nanoparticles or microparticles stabilize liquid drops, typically at microliter volumes [31]. On an even larger scale, granular materials such as dry sand (comprising particles with diameters of several hundred  $\mu\text{m}$ ) have been employed to encapsulate oil drops [32].

### 1.2.3 | Packaging Strategy

*Definition:* Packaging strategy here refers explicitly to the method, concept, or system used to primarily isolate the payload from its environment.

*Synonyms:* Commonly used terms include “encapsulation system” or simply “encapsulation” [33]; we use “packaging concept” and “packaging approach” as synonyms.

*Characteristics:* The packaging strategy is dependent on the intended application and the extent of interaction between the payload and its surroundings. For instance, scenarios involving reactive or sensitive payloads require complete sealing to prevent unwanted chemical alterations. An illustrative example is pharmaceutical products, where protection from moisture or oxygen is essential to maintain drug stability and efficacy [13, 34]. Conversely, certain applications demand controlled interaction with the environment, requiring semipermeable packaging. For example, also in a pharmaceutical context, the controlled release or targeted delivery of active ingredients are key elements in packaging strategies aiming at specific therapeutic effects [34]. In materials self-assembly, a notable example is the encapsulation of hydroxypropylcellulose solutions in liquid marbles, where controlled water extraction induces the formation of structurally colored liquid crystalline phases [35].

### 1.2.4 | The “Packaging Equation”

When designing a packaging strategy, the key characteristics of both the payload and packaging material must be considered, along with the interactions between them that dictate compatibility. At the same time, the desired characteristics of the packaging strategy (e.g., functionality, method, location of application) should be carefully considered. To provide a graphical illustration of the packaging strategy, which encompasses the above key terms and their inter-relation, we introduce the “packaging equation” (Figure 2). This is a conceptual representation of packaging as the sum of the payload and the packaging material.

### 1.2.5 | Packaging Versus Encapsulation

“Encapsulation” and “packaging” have both been used to indicate the isolation of the payload. Nevertheless, they often refer to distinct cases in terms of payload volume, as well as the structure and function of the packaging material. Encapsulation typically refers to micro- or nanoscale systems, often integrating advanced functionalities like controlled release, stability enhancement, or targeted delivery [33]. Examples include liposomes for drug delivery, microcapsules releasing fragrances, or gas microbubbles improving ultrasound imaging. In contrast, packaging generally pertains to macroscale containment, emphasizing protection, transportability, and practicality, often through multilayered systems like cartons protecting contents from mechanical stress, moisture, oxygen, and light [36]. For simplicity, we consider the two terms equivalent and use “packaging” for all cases of payload containment discussed.

## 1.3 | Types of Packaging Strategies Used for Payloads in Science and Engineering

This article focuses on packaging concepts explored in research and development activities. Hence, we primarily discuss research

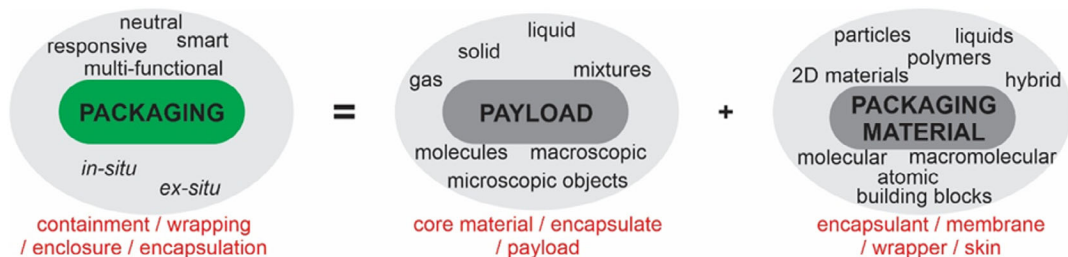


**FIGURE 2** | Schematic of the “packaging equation,” where packaging is the sum of the payload and the packaging material. Under the bubbles enclosing the equation terms, frequently used synonyms are included to provide a universal picture of packaging regardless of the specific terminology used. A few keywords are given within each bubble to provide a glimpse of the varying characteristics of the packaging strategy (e.g., functionality, location of application), the payload (e.g., physical state, composition), and the packaging material (e.g., type and length scale of building blocks).

conducted on a laboratory scale. Maintaining this focus, we describe in this section different categorizations of packaging solutions that can be made.

### 1.3.1 | Neutral, Multifunctional, and Responsive Packaging

Considering the functionality of a packaging strategy, we may identify three categories: neutral, multifunctional, and responsive packaging. Neutral packaging refers to the simplest form of containment, where the sole purpose is to physically isolate the payload from its environment. This provides basic payload protection without necessarily adding any extra functionality. An example is cellulose capsules for pharmaceuticals, where cellulose chains form a gel that physically isolates the active ingredients from the environment [13].

Multifunctional packaging goes beyond simple isolation by providing at least one additional functionality, e.g., controlled permeability, improved handling, transparency, or mechanical robustness. For instance, edible lipids enclosing liquids not only isolate the payload but also enhance visual aesthetics and facilitate controlled consumption [34, 37]. Similarly, “dry water,” encapsulated by silica nanoparticles, converts liquid water into a powder-like form, enhancing handling and transport convenience without chemically altering the cargo [38].

Responsive packaging strategies incorporate responsive behavior to internal (payload-related) or external (environment-related) stimuli. An illustrative example is liquid marbles containing structurally colored liquid crystals that respond dynamically to thermal, mechanical, or chemical stimuli [35] (responsive payload). Similarly, gas marbles stabilized by pH-responsive micro-particles enable controlled gas release, responding to pH changes [39] (responsive packaging material). When multiple functionalities are combined with responsiveness, one can envision the emergence of smart packaging, which represents the highest level of complexity and usability. This is a future direction we find very promising, discussed in Section 6.

### 1.3.2 | In-Situ and Ex-Situ Packaging

Packaging strategies may also be categorized based on the location of the packaging material with respect to the original location of the payload. In in-situ packaging, encapsulation occurs at the location where the payload is formed or used. Conversely, ex-situ packaging requires the payload to be transported to a separate location for encapsulation. An example of in-situ encapsulation is the

WRAPPINGS method, where liquid payloads are enclosed in thin poly(cyanoacrylate) films directly on-site via interfacial polymerization [24]. Other examples include graphene veils or polymer coatings grown directly on the payload surface, enabling precise, contamination-free packaging [40, 41]. Common ex-situ packaging platforms include liquid marbles, where liquid drops are typically placed onto powder beds to form packaged entities [31]. Another prominent example is “splash wrapping,” where liquid droplets fall onto polymer films to create packaged entities, involving transportation before encapsulation [42].

## 1.4 | Goal, Focus, and Structure of This Article

Packaging is a research and development theme at the heart of several industries, where applied disciplines like biotechnology, food science, pharmaceutical technology, and others cross paths with traditional disciplines dealing with materials, such as chemistry, physics, materials science, and engineering. This blending of interests, expectations, ways of thinking, and technical approaches makes the packaging challenge a particularly interesting one. At the same time, it may be intimidating, especially for newcomers who are exposed to a large variety of terms and concepts. The primary goal of this paper is to guide and inspire the reader, regardless of their background, so that informed decisions can be taken when a packaging strategy is considered. We aim to serve both newcomers and seasoned researchers by providing an analytical breakdown of the packaging system, using a universal language, and selecting examples that illustrate this purpose. This will enable the constructive combination of diverse expertise and mindsets to develop innovative packaging strategies.

This review focuses primarily on macroscopic (characteristic length  $>100\ \mu\text{m}$ , characteristic volume  $>1\ \text{pL}$ ), self-standing packaging solutions. While occasionally referring to smaller scales for context, our main intent is to clearly present, analyze, and unify the diverse yet crucial topic of macroscopic packaging [9]. Thus, we selectively discuss representative literature in-depth, aiming to provide a comprehensive, pedagogical, and standalone overview (Table 1). Emphasis is given to packaging materials based on soft matter, because we believe that soft materials are ideal for meeting the demanding requirements of packaging. Our own experience has shown us that it is currently possible to precisely engineer their properties and thus tailor their macroscopic behavior [69, 70]. This, in conjunction with their tendency to respond to small perturbations with a large

**TABLE 1** | The logic followed for the analysis of the selected literature. The various packaging strategies are grouped according to the payload physical state. Each strategy is accompanied by the (i) corresponding payload (and its typical -order of magnitude- volume), (ii) packaging material (and its characteristic -order of magnitude-dimension), (iii) key functional characteristics (based on the discussion in Section 1.3), and (iv) representative examples, analyzed in detail in the following sections.

Packaging strategy	Payload	Packaging material	Packaging functionality	Examples
Liquid marbles, liquid plasticines	Liquid (water, organics, complex fluids, liquid metals) (1–10 $\mu\text{L}$ )	Nanoparticles (10–100 nm), microparticles (10–100 $\mu\text{m}$ ), granular particles (100 $\mu\text{m}$ –1 mm), macroscopic particles (1 mm)	Neutral, functional (chemistry, photonics, sensing, edible), responsive (magnetic field, chemicals, pressure, temperature)	Water LMs [31] rapeseed oil LMs [43] galinstan LMs [44] cell culture LMs [45] water plasticines [46] polyhedral LMs [47] edible LMs [48]
Dry water	Liquid (water) (0.1–10 nL)	Nanoparticles (10–100 nm)	Neutral, functional (handling)	Powder-like dry water [38]
Particle monolayer destabilization	Liquid (organic) (100 $\mu\text{L}$ )	Granular particles (100 $\mu\text{m}$ –1 mm)	Neutral	Liquid packaging with granular rafts [32]
In-situ polymerization	Liquid (resins, ionic liquids) (1 $\mu\text{L}$ )	<i>In-situ</i> thin polymer films (10–100 nm thick)	Neutral, functional (optics), responsive (electric field); in situ	Reactive adhesives [49] varifocal liquid lenses [50]
Polymers in solution	Liquid (water, organics, comple fluids) (1–10 $\mu\text{L}$ )	Films of pre-synthesized polymer (1 $\mu\text{m}$ thickness)	Neutral, functional (lab-in-a drop); in situ	Polymer-wrapped drops [51] liquid pearls [52]
Hydrogels	Liquid (drugs in solution, complex fluids) (1–10 $\mu\text{L}$ )	<i>In-situ</i> physically x-linked polymers (1 $\mu\text{m}$ )	Neutral, functional (controlled release, lab-in-a-drop); in situ	Hydrogel spheres [53]
Polymer films	Liquid (water, organics) (1–100 $\mu\text{L}$ )	Self-standing polymer films (0.01–10 $\mu\text{m}$ thick)	Neutral, functional (reversibility); in situ	Capillary origami [54] splash-wrapping [42]
Metal films	Liquid (ionic liquid)	Continuous metal film (1 nm thick), nanoparticles (10 nm)	Neutral, functional (optics); <i>in-situ</i>	Ag-coated ionic liquid mirror [55]
Hybrid packages	Liquid (water, organics, solutions) (1 $\mu\text{L}$ )	Microparticles (100 $\mu\text{m}$ ) and polymer shell (100 $\mu\text{m}$ thick)	Neutral, functional (controlled release)	LMs coated with particles & polymers [56] drops stabilized with nanoparticle surfactants [57]
Solid nanocontainers	Liquid (aqueous & organic solutions) (0.1–1 nL)	Continuous metal and solder (10 $\mu\text{m}$ thick)	Neutral, functional (spatially controlled release and reactions), responsive (magnetic field)	Micromachined metal nanocontainers [58]

(Continues)

TABLE 1 | (Continued)

Packaging strategy	Payload	Packaging material	Packaging functionality	Examples
Liquid films	Liquid (organics)(10 µL)	Liquid layer(1 mm thick)	Neutral	Drop packaging with interfacial oil layer [59]
Long-lastin bubbles	Gas (air) (1 mL–1 kL)	Complex fluid layer (0.1–1 µm thick)	Neutral; in situ	Giant soap bubbles [10]
Gas marbles	Gas (air) (0.01–1 mL)	Microparticles-granular particles (1 µm–1 mm)	Neutral, functional (edible, controlled release), responsive (environment pH)	Air marbles [60] edible GMs [61]
Graphene films, graphene oxide films	Solids, micro- objects and liquid (particles, artworks, liquids, gases, bacteria) (1–100 µm)	Graphene/graphene oxide (1 nm thick)	Multifunctional (light/electron transparent, gas barrier, conformal), responsive (selective permeability)	Graphene veils for artwork [40] evaporation-driven interfacial membranes [43]
Clay-based films	Solid (fruits, vegetables) (mm–cm)	Clay particles, water-based clay composites (1 nm–10 µm)	Neutral, multifunctional (semi-perm., C <sub>2</sub> H <sub>4</sub> scavenger, disposable, controlled release); in situ	Fresh produce preservation [62, 63] drug loading & release [64]
Cellulose-based coatings	Solid (roots, fruits, paper) (0.1–10 cm)	Cellulose nanomaterials (1 nm–1 µm)	multifunctional (semi-permeable, antioxidant, pH, responsive); <i>in-situ</i>	Paper preservation [65] food preservation [66]
Foam marbles	Liquid (foam), gas (air) (100 µL and 0.1–1,000 nL)	Nanoparticles (100 nm)	Neutral	Foam marbles [67]
Capillary containers	Liquid (water, organic, drug in solution), gas (air) (10–100 µL)	Macroscopic resin frame and metal microbeads (100 µm)	Neutral, functional (capture and release, microfluidics, chemistry), responsive (magnetic field)	Magnetic capillary containers [68]
WRAPPINGS	Liquid (water, solutions, compl. fluids), gas (air, CO <sub>2</sub> , reactive), solid (flat and curved)(1 µL–10 mL)	In-situ thin polymer films (1 nm–10 µm)	Neutral, functional (lab-in-a-drop, lab-in-a bubble, controlled release); in situ	WRAPPINGS [24]

response function [35], may be exploited to develop packaging materials highly responsive to both internal (payload-originated) and external stimuli. This capability may be further extended to incorporate smart features, such as unsupervised yet appropriate response to changes in their environment [71, 72]. While these elaborate features are key for research and development settings, the fact that many soft materials are abundant, cost-effective, sustainable, and recyclable makes them promising candidates for scaling up.

This review is structured as follows: After this introduction of fundamental concepts and terminology, we categorize packaging strategies according to the physical state of the payload. Based on this, we analyze the packaging of liquid (Section 2), gaseous (Section 3), solid (Section 4), and multiple (Section 5) payloads. Each category is supported by illustrative examples chosen for clarity, relevance, and practical applicability. In Section 6, multifunctional and responsive packaging strategies are discussed. In Section 7, we highlight recent innovations, current limitations, and prospective future directions, before conclusions (Section 8).

## 2 | Packaging of Liquid Payloads

Numerous strategies have been developed for packaging liquids, usually aiming to [56] (i) shield the payload from thermal, pH, and oxidative stresses; (ii) mask odors; (iii) prevent chemical reactions with the environment; (iv) enable controlled payload release; and (v) convert liquids into solid-like forms for easier handling [38]. Some selected strategies are discussed below.

### 2.1 | Particles as Packaging Material

The following discussion focuses on *self-standing* liquid entities that are packaged using particles of various sizes, from nanoparticles to granular materials. Other cases of particle-based liquid packaging within a liquid environment (e.g., bicontinuous, interfacially jammed colloidal emulsion gels [73]), although interesting and useful, are not discussed here.

#### 2.1.1 | Liquid Marbles

A prominent platform for encapsulating macroscopic liquid volumes, which has received vivid interest over the last 25 years, is liquid marbles (Figure 3A). These are sessile drops coated by particles exhibiting poor wettability with respect to the enclosed liquid [31]. The large contact angle at the particle–liquid–gas contact line implies partial immersion of the particle in the liquid, with the remainder exposed to the surrounding phase. This particle shell prevents direct contact between the enclosed liquid and a substrate (typically, but not limited to, a solid); consequently, the enclosed liquid can be transported without wetting the substrate. Besides non-wetting behavior, liquid marbles exhibit other unusual properties, such as resistance to mechanical shocks during impact and extremely low friction when rolling on solid surfaces [75].

Much of the “exotic” behavior of liquid marbles is due to the strong attachment of particles at the fluid interface. The particle size and structural features of the interfacial particle assemblies (the packaging material) are critical because they directly affect the macroscopic properties of liquid marbles, such as mechanical

stability [76] and optical transparency [77]. The adsorption energy of a particle with radius  $a$  at the fluid interface is  $E_{ads} = \pi a^2 \gamma (1 \pm \cos \theta)^2$ , where  $k_B$ ,  $T$ , and  $\gamma$  are Boltzmann’s constant, temperature, and interfacial tension, respectively [78]. For a particle of diameter 100 nm forming a contact angle  $\theta = 90^\circ$  at the air–water interface,  $E_{ads} \sim 10^5 k_B T$ . The resulting stability is further enhanced by additional particle layers that usually adhere onto the monolayer coating the drop. A wide variety of particles have been used to prepare liquid marbles [79]. These include nanoparticles, such as fumed silica (200–500 nm long aggregate chains of primary particles) [77] and magnetic  $Fe_3O_4$  nanoparticles (diameter  $\sim 10$  nm) [80], as well as microparticles, either from natural resources like lycopodium ( $\sim 20 \mu m$ ) [31] or synthetic like graphite (2–30  $\mu m$ ) [81] and poly(styrene) (15–100  $\mu m$ ) [76].

Particle surface chemistry is also of key importance because it defines what kind of liquid payloads can be enclosed. Liquid surface tension directly influences  $E_{ads}$  and thus liquid marble stability. Numerous simple and complex liquids of varying  $\gamma$ , both aqueous and non-aqueous, have been enclosed within liquid marbles to produce self-standing packages [79, 82]. Early papers reported on water and water/glycerol liquid marbles [75]. Other payloads include vegetable oils (Figure 3A, i) and organic solvents (encapsulated by perfluorooctanoic acid-modified  $TiO_2$  nanoparticles,  $\sim 470$  nm) [43], ionic liquids (enclosed by oligomeric ( $< 1 \mu m$ ) or polymerized (up to 35  $\mu m$ ) tetrafluoroethylene [74] (Figure 3A,ii), and complex fluids like concentrated polymer solutions [35] and aqueous phases containing cancer cells [83]. Less common payloads like liquid metals have also been packaged using  $WO_3$  nanoparticles (size  $\sim 80$  nm) [44] (Figure 3A,iii).

The basic function of a liquid marble is to separate the core liquid from the surrounding environment. Beyond neutral packaging, liquid marbles have been used as packaging platforms featuring additional functionalities. Their non-wetting transport, combined with being external field-addressable (e.g., magnetic, optical, electric) [80, 84–95] has led to applications in microfluidics [96, 97] and materials science [98], while a plethora of green applications has emerged [99]. A remarkable example is liquid marbles stabilized by magnetic  $Fe_3O_4$  nanoparticles as miniature reactors for various reactions (e.g., chemiluminescence, acid–base, nanoparticle synthesis), either via the coalescence of two reactant-laden liquid marbles or within a single marble. These systems can also integrate purification and analysis: by opening the liquid marble with a magnetic field, the product can be retrieved for spectroscopic characterization [85]. Liquid marbles have also been exploited for making functional materials from microscopic building blocks in a non-chemical, bottom-up fashion. Gu et al. fabricated marbles containing monodisperse  $SiO_2$  nanoparticles and a photosensitive polymer precursor, coated with trimethylolpropane triacrylate microparticles. Exposing the core liquid to UV light and subsequent ultrasonication resulted in spheres with non-iridescent structural color, arising from colloidal crystallization [100]. Another example of exploiting the packaging material properties was shown by Tian et al., who utilized liquid marbles as respirable bioreactors for preparing cell cultures. The anaerobic *Lactococcus lactis* subsp. *Cremoris* and the aerobic *Saccharomyces cerevisiae* microorganisms were incubated in liquid marbles stabilized with poly(tetrafluoroethylene) microparticles (100  $\mu m$ ) (Figure 3A,iv–v). Compared with the bulk liquid structure under identical

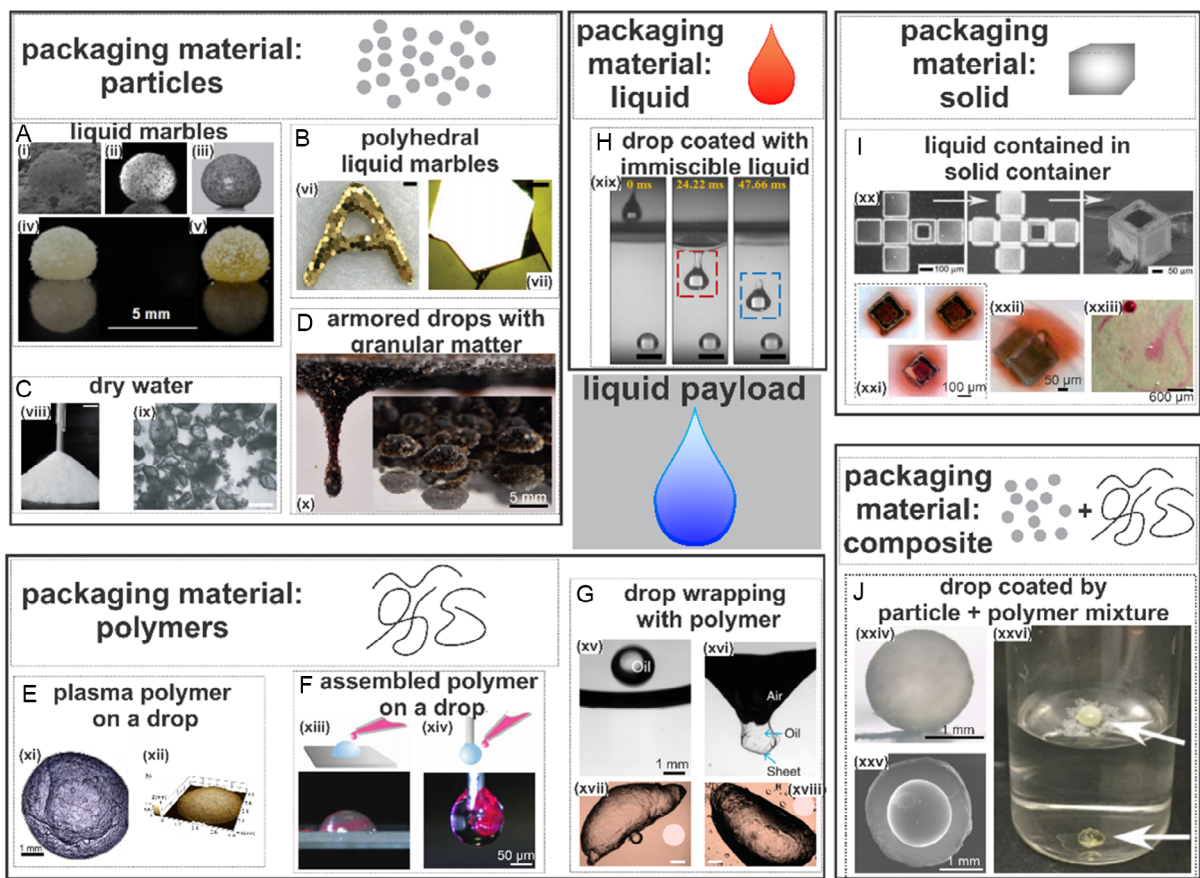


**FIGURE 3** | Packaging of liquid payloads. Each panel shows various packaging materials comprised of particles, polymers, immiscible liquids, metals, and hybrids. (A) Liquid marbles enclosing (i) rapeseed oil using  $\text{TiO}_2$  nanoparticles. Adapted with permission [43]. Copyright 2011, Taylor and Francis. (ii) the ionic liquid 1-ethyl-3-methylimidazolium tetrafluoroborate using oligomeric tetrafluoroethylene particles. Adapted with permission [74]. Copyright 2007, American Chemical Society. (iii) the liquid metal Galinstan using  $\text{WO}_3$  nanoparticles. Adapted with permission [44]. Copyright 2012, Wiley, (iv-v) cultures ( $20\ \mu\text{l}$ ) of *L. cremoris* (iv) and *S. cerevisiae* (v) using poly(tetrafluoroethylene) microparticles. Adapted with permission [45]. Copyright 2013, Elsevier. (B) Polyhedral liquid marbles representing complex-shaped water packages, where the packaging material comprises macroscopic poly(ethylene terephthalate) plates. Scale bars are 5 mm and 0.5 mm, respectively. Adapted with permission [47]. Copyright 2019, Wiley. (C) “Dry water,” a powder-like material allowing for easy handling of tiny water packages, e.g., passing through a funnel (viii). These water packages comprise droplets coated with fumed silica nanoparticles dispersed in air (ix). Scale bars are 1 cm and  $200\ \mu\text{m}$ , respectively. Adapted with permission [38]. Copyright 2006, Springer Nature. (D) The destabilization of a sand particle raft sitting on a motor oil layer on seawater leads to motor oil packages enclosed by the granular particles (x), which sink onto the bottom of the water column (inset). Adapted with permission [32]. Copyright 2013, Springer Nature. (E) Packaging of a thiol-(meth)acrylate-epoxy drop with a polymer film by atmospheric pressure plasma polymerization. Confocal micrograph (xi) and corresponding topography (xii) of the film. Adapted with permission [49]. Copyright 2020, Wiley. (F) Packaging of sessile (xiii) or pendant water drops (xiv) with a self-assembled film formed by spreading poly(lactic-co-glycolic acid)/dimethyl carbonate solution onto the liquid payloads. Adapted under the terms of the CC BY license [51]. Copyright 2019, American Association for the Advancement of Science. (G) A fluorocarbon oil drop landing onto a poly(styrene) film floating on water (xv) is enclosed by the film upon impact (xvi). A water drop packaged with this splash wrapping method in hexadecane (xvii); this package could even be extracted into air (xviii). The scale bars are 0.5 mm. Adapted with permission [42]. Copyright 2018, Springer Nature. (H) Packaging of an oil drop by a layer of an immiscible oil. Time-lapse images showing the entry of a laser oil drop into an aqueous bath, after passing through a canola oil layer on the free surface of water. Scale bars are 4 mm. Adapted with permission [59]. Copyright 2020, Elsevier. (I) Liquid packaging using multi-functional microcontainers from self-organized 2D metallic templates (xx). Isotropic (xxi) and anisotropic (xxii) release of an enclosed dye in the surrounding liquid, achieved by engineering container porosity. A spatially controlled chemical reaction across a G-shaped trajectory enabled by incorporating magnetic functionality into the container (xxiii). Adapted with permission [58]. Copyright 2006, American Chemical Society. (J) Liquid packaging with a hybrid particle-polymer packaging material. A compound liquid marble comprising monomer/initiator mixture and a water droplet, coated with silicon monolith, yields a solid capsule enclosing the aqueous payload (xxiv: side view, xxv: cross-section). xxvi). The capsules sink in water (bottom) after removing excess coating powder (top). Scale bars are 1 mm. Adapted with permission [56]. Copyright 2018, Elsevier.

conditions, the marble environment provided a faster and slower proliferation rate for the aerobic and anaerobic microorganisms, respectively, attributed to  $\text{O}_2$  and  $\text{CO}_2$  transport through the coating [45].

### 2.1.2 | Liquid Plasticines and Dry Water

Li *et al.* fabricated “liquid plasticines,” macroscopic materials the shape of which can be designed at will. To produce a liquid plasticine, a drop is pressed against two plates coated with a

200–300 nm thick layer of xerogel of hydrophobic silica nanoparticles (diameter  $\sim$  20 nm). The weak interparticle interactions in the xerogel allow particle transfer onto the liquid surface, yielding a flattened drop. After removing the compressive force, interfacial jamming prevents shape recovery and arrests the drop shape, yielding a stable, elongated drop in air. By joining nanoparticle-decorated drops together and adding more water into the merged structure, a liquid plasticine is formed. Notably, there is no limit to the final volume of the liquid plasticine, because the procedure can be repeated many times. Liquid plasticines with designable shapes and high optical transparency have been demonstrated. These multifunctional packages may find use as liquid lenses or channel-like containers for (bio)chemical manipulations [46].

Geyer et al. used mm-sized, hexagonal poly(ethylene terephthalate) plates (thickness 40–55  $\mu$ m) to fabricate polyhedral liquid marbles (Figure 3B). Upon contact with a drop, plates spontaneously adsorb at the air–water interface and assemble into a 2D structure, packaging the payload. The structural characteristics are defined by the ratio of plate to drop diameter. For drops with diameters significantly larger than the plate size (drop volume  $\sim$  60  $\mu$ L), the relatively small curvature of the drop free surface allows plates to fully attach onto the interface, resulting in spherical liquid marbles with hexagonally packed domains. For drop diameters comparable to the plate size ( $\leq$  30  $\mu$ L) and for large plates, the high curvature forces the plates tangent to the free surface, partially protruding out of the fluid interface. Further volume reduction ( $\sim$ 15  $\mu$ L) resulted in marbles with different shapes, such as tetrahedra, pentahedra, and cubes. High- $\gamma$ , non-aqueous liquids like glycerol and diiodomethane were also enclosed in polyhedral liquid marbles. Interestingly, spherocylindrical marbles with a large aspect ratio ( $>$ are10) could be made by either merging polyhedral marbles, removing liquid, or adding excess plates on a given marble and deforming it (Figure 3B,vi). Inhomogeneous mechanical stresses were used to make dumbbell- and letter-shaped liquid marbles. This plastic behavior was attributed to the steric jamming of the plates at the interface (Figure 3B,vii). Due to their macroscopic size, PET plates feature adsorption energies more than three orders of magnitude higher than those for marbles stabilized with microparticles, providing a strong packaging material. Polyhedral liquid marbles show potential as sensors, because they respond to chemical stimuli (e.g., exposure to ammonia or tetrahydrofuran) [47].

Binks and Murakami showed the phase inversion of particle-stabilized air-water systems, from air-in-water foams, to water-in-air systems, and vice versa. This was achieved either by progressively decreasing the wettability of particles (silanized fumed silica nanoparticles) at a fixed air/water ratio or by varying the air/water ratio at fixed particle wettability. Starting from a stable air-in-water foam (near the phase inversion boundary) and following the first route, the authors produced “dry water.” This is a water-in-air system that, macroscopically, is powder-like and free-flowing (Figure 3C,viii). Microscopically, it contains numerous nanoparticle-coated water droplets (diameters 50–400  $\mu$ m); most of them are nonspherical because the jammed particle layer at their surface prevents relaxation (Figure 3C,ix). Whereas no water separation occurred when this powder was kept in a closed vessel, water was released by applying shear (e.g., by rubbing the material between the fingers). Following the second route, from a stable air-in-water foam (close to the inversion boundary), a

“soufflé-like” material, also comprising nanoparticle-stabilized droplets in air, formed for a range of water volume fractions. Compared with dry water, the constituent macroscopic particles are more aggregated and stickier, with the material showing a spongy nature. Both dry water and soufflé-like materials are macroscopic materials with fascinating properties that represent novel ways of packaging and releasing aqueous liquids [38].

### 2.1.3 | Drop Packaging with Particles Residing at a Fluid Interface

Abkarian et al. developed a packaging method relying on granular matter to isolate and transport organic liquids. In this process, a layer of oil (e.g., silicone or mineral oil) was deposited on water (denser than the oil), and large particles (e.g., ZrO<sub>2</sub>, diameters 350–700  $\mu$ m) were sprinkled onto the oil. Long-range capillary attractions between particles yielded a monolayer particle raft at the oil–water interface. When the particle number was sufficient, the monolayer became unstable: as the raft sank to the bottom of the aqueous phase, it wrapped itself around a volume of the oil phase, enclosing it. The significant weight of the particle armor is critical, as opposed to liquid marbles [31] and colloidal armored droplets [101], where the weight of coating particles is negligible. Two types of packaging scenarios were observed, depending on particle size and density. The first one was a single droplet enclosed by particles, whereas the second one was a particle-laden liquid jet destabilized by a Rayleigh-Plateau-like instability, producing several encapsulated droplets. The typical droplet diameters were on the order of millimeters. This method was tested as a sustainable, non-chemical strategy for containing oil spills. Dry sand was placed on a motor oil layer floating on seawater that, upon raft destabilization, resulted in particle-decorated motor oil droplets that sedimented and remained intact within the aqueous phase (Figure 3D, x) [32].

## 2.2 | Polymers as Packaging Material

Polymers enable conformal coatings with tunable thickness, permeability, and optical properties. They may be formed directly at the payload surface via polymerization or used as pre-made films to produce durable, self-supporting liquid containers, as we discuss below.

### 2.2.1 | Polymer Films via Interfacial Polymerization

Rezaei et al. employed atmospheric pressure plasma to form free radicals and initiate polymerization of the topmost layer of a reactive liquid droplet containing unsaturated C=C bonds. This resulted in a polymer skin on the droplet surface (Figure 3E), which prevented the underlying reactive liquid from interacting with plasma species, thereby protecting it from further reactions. The authors demonstrated examples where sessile droplets (volume  $\sim$  3  $\mu$ L) of resins (acrylates and thiol acrylates) and catalysts were enclosed by a polymer film (thickness  $\sim$  50 nm). This packaging material enabled the confinement of the reactive payload on the supporting substrate in a nonreactive state. Pressing two substrates against each other led to the release of the adhesives and the formation of a strong bond [49].

Haller et al. introduced an ionic liquid substrate into an initiated Chemical Vapor Deposition process. Monomer and initiator vapors were introduced in a reaction chamber containing a

silicon wafer with sessile drops (5  $\mu\text{L}$ ) of 1-butyl-3-methylimidazolium hexafluorophosphate placed on it. The location of polymerization (i.e., liquid-gas interface, solid-gas interface, and liquid bulk) and, in turn, the characteristics of the formed polymer depended on the reaction conditions and monomer solubility in the ionic liquid. For the soluble monomer 2-hydroxyethyl methacrylate, polymerization occurred in all three locations. For short reaction times, a polymer film partially covered the drop and it could be lifted off and kept self-standing. Longer reaction times led to a polymer film fully enclosing the ionic liquid drop. The film thickness at the drop center was larger than near the edge, because chains were grown both at the liquid-gas interface and the ionic liquid bulk. When the insoluble monomer 1H, 1H,2H, 2H-perfluorodecyl acrylate was used, polymers formed only at the liquid-gas and solid-gas interfaces, yielding a skin that packaged the drop completely. The more uniform thickness compared to the poly(2-hydroxyethyl methacrylate) film suggested that polymerization started and proceeded evenly across the ionic liquid surface. This work highlighted the potential to develop composite polymer-ionic liquid materials with controlled structure, potentially useful as electrolyte membranes in fuel cells and nonvolatile electrolytes in batteries [102].

### 2.2.2 | Films from Presynthesized Polymers in Solution

Coppola *et al.* developed a bottom-up method for the *in situ* packaging of liquid payloads, based on the self-assembly of biocompatible polymers (in solution) into a film following the water profile. In the simplest case, a droplet of poly(lactic-co-glycolic acid) solution in dimethyl carbonate was placed onto a sessile water drop sitting on a solid substrate. The polymer solution wrapped the water surface, driven by the reduction of the total interfacial energy. Dimethyl carbonate was slowly extracted by the aqueous phase, and the poly(lactic-co-glycolic acid) chains spread over the water surface. Within seconds, a homogeneous, nonporous film acted as an adaptive suit and encased the entire sessile drop (Figure 3F,xiii); pendant drops could be packaged similarly (Figure 3F,xiv). The polymer membranes (thickness  $\sim 1.65 \mu\text{m}$ ) were transparent to visible light, had low water vapor permeability (140 (g  $\mu\text{m}$ )/( $\text{m}^2 \text{ day kPa}$ ), and very high oxygen permeability (1.9  $\times 10^{-5}$  ( $\text{cm}^3 \mu\text{m}$ )/( $\text{m}^2 \text{ day atm}$ )). These properties allowed *in vitro* lab-in-a-drop experiments involving the observation of aqueous payloads containing *Caenorhabditis elegans*, a model organism for investigating neuron systems. Although polymer membrane formation led to a marked decrease in the microorganisms movement (presumably due to geometrical constraints and dimethyl carbonate presence), this was reversible, with microorganisms recovering their motility once the membrane was removed [51].

Bremond *et al.* produced “liquid pearls,” millimeter-sized drops of aqueous or oil phase packaged with a polymeric shell, employing a two-step microfluidic process. Initially, a compound pendant drop comprising the core liquid (water or oil, radius 1.8–2.2 mm) and a surrounding shell of aqueous sodium alginate solution (thickness 0.6–150  $\mu\text{m}$ ) was created in air, using two coaxial tubes in a dual dripping regime. In the second stage, after the breakup, the drop was immersed in an aqueous  $\text{CaCl}_2$  bath.  $\text{Ca}^{2+}$  ions diffused into the alginate solution and, by bridging adjacent polymer chains, yielded a 3D hydrogel network. For successful production, two key instabilities had to be suppressed. For aqueous cores, mixing with the surrounding aqueous phases was

prevented using surfactants that transformed the drop surface into a transient elastic membrane. For oil cores, suppression of dewetting of the aqueous film surrounding the hydrophobic drop was also ensured. This is activated by the recoiling of a thin thread produced by the pinch-off of the compound drop and defines the minimum shell thickness. A setup with three coaxial tubes was used to introduce aqueous glucose solution; this additional liquid layer protected the outer alginate layer from divalent ions in the core liquid, which consisted of yeast cells and culture medium. This test was successful, as evidenced by the reproduction of cells within the liquid pearl [52].

Inspired by the Lotus leaf effect, Song *et al.* developed a simple method for packaging active molecules and living cells in spherical hydrogels or solid polymer particles, which served as reservoirs for delivery and release. In a typical experiment, an aqueous polysaccharide solution drop ( $\sim 2\text{--}20 \mu\text{L}$ ) was placed onto a superhydrophobic substrate (based on silanized poly(styrene)), and  $\text{CaCl}_2$  solution was used to crosslink the polymer chains *in situ*. Theophylline, a water-soluble drug, was also introduced into the liquid payload. The resulting spherical alginate hydrogels (diameter  $\sim 1\text{--}2 \text{ mm}$ ) had a very high drug encapsulation efficiency, because no theophylline was lost onto the substrate during the packaging process. Release experiments indicated that  $\sim 100\%$  of the incorporated theophylline diffused into an aqueous environment. Payloads containing living cells were also packaged using this method. Alginate drops carrying L929 cells were prepared on a superhydrophobic surface and crosslinked using  $\text{CaCl}_2$ . Fluorescent microscopy observations indicated that the living cells were homogeneously distributed within the (cross-linked) volume of the hydrogel spheres [53].

### 2.2.3 | Prefabricated Polymer Films

Liquid payloads can also be packaged using prefabricated films of insoluble polymer, such as films supported by solid or liquid (nonsolvent) substrates. Py *et al.* exploited the interaction between polymer elasticity and water capillarity to generate drops packaged by polymers, via a “capillary origami” process. In a typical experiment, a water drop (1–80  $\mu\text{L}$ ) was deposited on a poly(dimethylsiloxane) film (thickness 40–80  $\mu\text{m}$ ) placed on a superhydrophobic substrate. Upon evaporation, the surface tension force led to a continuous curvature increase of the sheet. When the sheet was sufficiently thin, it enclosed the liquid; conversely, the increased stiffness of thick films did not allow for sufficient film bending to achieve complete closure. Liquid enclosure was not possible below a critical length scale. This so-called elastocapillary length scales as the film thickness  $d^{3/2}$ ; thus, thinner sheets result in much smaller critical lengths, which is favorable to miniaturization. Interestingly, the 3D shape of the resulting liquid package was defined by the initial (i.e., 2D) shape of the planar polymer sheet. Starting from respectively flower-like and cross-shaped structures, approximately spherical and cubic liquid packages could be fabricated, highlighting the possibility to engineer the final closed state [54].

Kumar *et al.* exploited the impact dynamics of a droplet landing on an ultrathin polymer film floating on a second (immiscible) liquid. In a typical experiment, an oil drop (e.g., fluorinated oil, radius 0.6–1.2 mm) was dropped onto a poly(styrene) film (thickness 46–372 nm) residing at the surface of a second liquid (water, Figure 3G,xv). When the kinetic energy of the droplet was

sufficient to overcome the interfacial energies involved, it separated from the air-water interface and was packaged by the polymer sheet (Figure 3G,xvi). By modulating the 2D film shape, the 3D shape of the enclosed droplet could be tailored, as evidenced by sphere, half-sphere, tetrahedron, or cube-like liquid packages. This “splash wrapping” method featured almost perfect seams: the film edges were neither overlapping nor far apart, showing no openings. The encapsulation was reversible, evidenced by the possibility to open the package to release the enclosed liquid or its ability to reform after mechanical perturbation. The versatility of this method was illustrated by packaging hydrocarbon oil and aqueous drops in ethanol and oil environment, respectively. Liquid packages could even be extracted into air (Figure 3G,xvii-xviii). To avoid degradation of the polymer by the involved liquids, bilayer films of poly(styrene) and Cytop were utilized [42].

### 2.3 | Liquid Packaging With Liquids

Misra *et al.* demonstrated a method for packaging droplets of a core liquid with a shell of a second liquid in a host (third) liquid, based on surface energy minimization. A shell liquid (canola oil) was deposited onto the host liquid (water), and a droplet (~15.5  $\mu\text{L}$ ) of core liquid (silicones mixed with polyphenol ethers) was dropped onto the interface. Two conditions were necessary for successful wrapping of the core droplet by the shell liquid. First, shell formation around the core liquid must be thermodynamically favorable:  $\gamma_{\text{core-shell}} + \gamma_{\text{shell-host}} < \gamma_{\text{core}}$ , where  $\gamma_{\text{core-shell}}$ ,  $\gamma_{\text{shell-host}}$ ,  $\gamma_{\text{core}}$  are the interfacial tensions of the core liquid-shell liquid, shell liquid-host liquid, and core liquid-air pairs, respectively. This is necessary but not sufficient; the core droplet must also possess enough kinetic energy to overcome the interfacial energy barrier, while compensating for viscous dissipation during penetration of the interfacial layer of the shell and host liquids. For a given impact height and shell layer thickness (~2–2.8 mm), encapsulation occurred only above a critical droplet size. This method enabled stable packaging of an ethylene glycol droplet miscible with host water: the canola oil shell prevented dissolution while preserving droplet integrity (Figure 3H) [59]. Recent experiments utilized a hydrophobic loop at the bath surface to anchor the shell-forming liquid, eliminating the density constraint and limiting lateral spread, resulting in thicker interfacial lenses from the same volume [103].

### 2.4 | Liquid Packaging With Metals

Leong *et al.* developed a multifunctional system for packaging and delivery of tiny liquid payloads based on metallic microcontainers. A 2D metallic (e.g., Cu-based) template comprising solder hinges was fabricated by photolithography. Upon heating above the solder melting point, surface tension drove self-organization into a 3D hollow polyhedral structure (Figure 3I,xx). This way, containers of different shapes (e.g., cubes and pyramids) and volumes (230 pL–8 nL) were fabricated in a highly parallel process. Furthermore, patterning of one or more faces of the container with monodisperse pores of varying diameter was possible by photolithography. By adjusting the porosity, the release profile of the packaged payload was engineered. A spatially isotropic material release was documented for containers with identical porosity on all faces (Figure 3I,xxi), whereas

different pore sizes on different faces led to anisotropic release (Figure 3I,xxii). To impart magnetic functionality, Ni was used as packaging material. This enabled the demonstration of a spatially controlled chemical reaction, where phenolphthalein (pH indicator) was released into an alkaline solution in an arbitrary trajectory (Figure 3I,xxiii). Other spatially localized reactions were also shown with multiple containers [58].

### 2.5 | Hybrid Films as Packaging Material

The integration of particles within a polymer matrix enhances toughness and allows permeability regulation, while maintaining the overall mechanical integrity of the material. This can be used for making hybrid packaging materials with customizable release profiles. Takei *et al.* developed a liquid packaging strategy employing a particle-polymer packaging material, based on photopolymerizable liquid marbles. Matrix-type capsules with the liquid payload distributed in a continuous matrix were prepared by rolling a monomer drop containing photoinitiator (5  $\mu\text{L}$ ) on superamphiphobic powder (silicon monolith, particle size < 600  $\mu\text{m}$ ). The liquids of interest (tetradecane,  $\alpha$ -tocopherol, linalyl acetate, and doxorubicin dissolved in dimethyl sulfoxide) were also mixed with the monomer. White light-induced polymerization yielded solid marbles that enclosed the payload with efficiencies exceeding 99%. Core-shell capsules were prepared by first forming a monomer/initiator liquid marble (8  $\mu\text{L}$ ), injecting an aqueous droplet (2  $\mu\text{L}$ ) into it, and then solidifying it using light. To achieve highly spherical liquid marbles with shells of uniform thickness, a centrifugal force was applied that caused the denser monomer to move toward the liquid marble surface and the aqueous phase to move toward its center (Figure 3J,xxiv-xxv). By removing excess coating particles, the hybrid marbles sank in various liquids (Figure 3J,xxvi). Fluorescein sodium loaded into the aqueous payload was not released during a 7-day test. When poly(ethylene glycol) was incorporated into the shell, the release rate of the dye increased (up to 100% for the same period) with increasing poly(ethylene glycol) concentration, attributed to water channels formation in the shell [56].

Cui *et al.* explored the in-situ generation of nanoparticle surfactants at a water-oil interface and their use in stabilizing non-spherical water drops (typical size ~a few mm). An aqueous drop containing anionic nanoparticles (e.g., carboxylated poly(styrene)) was suspended in oil containing polymers with a cationic end group (e.g., amine-terminated poly(dimethylsiloxane)). Polymers were first assembled at the fluid interface, followed by diffusion of nanoparticles to the interface. Electrostatic attraction between the oppositely charged species resulted in nanoparticle surfactants, which reduced the interfacial energy and led to a jammed structure. By applying an electric field, the drop deformed and its surface area increased, resulting in unjamming of the nanoparticle surfactant assembly; this enabled the generation and interfacial assembly of additional nanoparticle surfactants. When the field was turned off jamming occurred once again, trapping the drop in an out-of-equilibrium shape. Unjamming of nanoparticle surfactants occurred locally, allowing for deformation of the drop interface in different directions. As a result, various shapes like tubes, fish-shaped structures, and complex anisometric structures (e.g., glass wool-like) formed. The electrostatic interactions between polymers and nanoparticles exceeded thermal energy and thus stabilized the nanoparticle surfactants at the interface.

Stability was further increased with difunctional polymers that bridged neighboring nanoparticles, yielding a crosslinked interfacial structure [57].

### 3 | Packaging of Gas Payloads

Microscopic gas packages find application in numerous industrial products. Although this research area is not the focus of this article, we briefly discuss a few representative examples and point to relevant reviews. Gas microbubbles (typical diameters one to a few micrometers) are used in products that enhance the signal in ultrasound examination. Besides imaging, focused ultrasound beam can destabilize microbubbles carrying active ingredients, enabling local delivery of drugs or genes [104]. Typically, lipids, proteins, and polymers are the packaging materials, and payloads are air, nitrogen, or perfluorocarbons [105]. Foams featuring a dispersed gas phase (bubbles) in a continuous (solid or liquid) phase are utilized in popular foods and drinks (e.g., ice cream, whipped cream, bread, cake, carbonated beverages). This aerated structure (bubble sizes  $\sim 10\text{--}100\ \mu\text{m}$ ) imparts desirable texture, while replacing fat particles with gas yields healthier products [106]. Most foam food products comprise air, nitrogen, or  $\text{CO}_2$  packages enclosed by packaging materials often based on solid particles. In such Pickering foams, proteins (and protein aggregates), nanoparticles (e.g., based on starch or cellulose), or microparticles (e.g., microgels) stabilize bubbles in a continuous phase (typically an aqueous solution) [107]. Contrarily, the packaging of macroscopic gas payloads has comparatively received less attention. Below, we review selected examples of this largely unexplored yet potentially useful area.

#### 3.1 | Macroscopic Gas Bubbles

A familiar example of gas packaging is a bubble stabilized in air by a thin liquid film. This packaging material is inherently fragile, severely limiting the utility of this packaging strategy. For pure liquid films, bubble lifetime is proportional to viscosity: bubbles covered with a polymer melt last much longer than water-enclosed bubbles (typical lifetime  $\sim\text{s}$ ). Here, bubble destabilization occurs due to the thinning of the liquid film down to thicknesses on the order of tens of nanometers, caused by gravity-driven liquid drainage [108]. Surfactants significantly increase the stability of bubbles enclosed by an aqueous film, with the lifetime of the resulting soap bubble depending on surfactant concentration. For intermediate concentrations, a complex interplay between gravity and capillary-driven drainage, Marangoni flows due to surfactant concentration gradients, and water evaporation dictates film stability. At high concentrations, the film becomes more rigid and some of these effects are suppressed; however, water evaporation and the presence of nuclei may also trigger bubble rupture [109].

#### 3.2 | Giant and Long-Lasting Soap Bubbles

Although soap bubbles are generally ephemeral structures, some interesting observations hint at their packaging potential. Introducing additives (e.g., glycerol) to the bubble solution drastically increases packaging material stability and thus the lifetime of soap bubbles (Figure 4A,i-ii). A more intriguing observation is the creation of giant soap bubbles (Figure 4A,iii): free-floating bubbles

with a volume of  $\sim 100\ \text{m}^3$  (surface area and diameter of  $\sim 100\ \text{m}^2$  and  $\sim 6\ \text{m}$ , respectively) have been recorded [10]. Giant soap bubbles in a sessile configuration (Figure 4A,iv) have also sparked scientific interest [110]. Although their geometrical features are impressive on their own, the structural characteristics of giant bubbles are even more remarkable: The thin-film interference color shows that the stabilizing film is only a few  $\mu\text{m}$  thick [10].

Besides giant bubble formation, which has enabled a vibrant and resourceful community of enthusiasts [112], these objects have attracted vivid research interest. Frazier et al. studied the rheology of bubble solutions comprising water, surfactants (dish detergent or sodium dodecyl sulfate), and high-molecular weight polymers (guar, a lubricant containing poly(ethylene oxide) and sucrose, or pure poly(ethylene oxide)). A right balance between the extensional properties counteracting film thinning and breaking, and sufficient flow to continuously draw liquid into the film was required. Bubbles also had to have a significant lifetime, not compromised by water evaporation and gravity-induced drainage. Polymers provided the appropriate rheological properties and increased longevity. Intermediate polymer concentrations and increased molecular weight dispersity led to optimal solutions for stable soap bubbles. This was attributed to the extensional rheological behavior of isolated chains and cooperative interactions between chains of varying lengths. Regardless of the exact formulation, bubble lifetime increased with increasing humidity, reaching a maximum at  $\sim 75\%$ . Above this value, lifetime increased further, with a fivefold increase at  $90\%$  compared with  $\sim 45\%$  humidity [10]. Such studies provide quantitative guidelines for preparing mechanically robust soap bubbles.

Although long-lasting bubbles are sensitive to drying and destabilization upon contact with almost any surface, they can provide a template for creating solid, long-lasting structures. This intriguing possibility was demonstrated by Jampani et al., who used free-standing and sessile soap bubbles as templates for the interfacial polymerization of cyanoacrylates. The result was robust polymeric films, serving as Do-It-Yourself chambers for storing and handling gaseous payloads or performing other tasks, as discussed in more detail in Section 6 [24].

#### 3.3 | Particle-Coated Bubbles: Gas Marbles

Timounay et al. introduced gas marbles, an interesting concept for packaging gaseous payloads (volumes  $\sim 100\ \text{mm}^3$ ) in air. To produce gas marbles, a solid frame was inserted into an aqueous surfactant solution covered with granular poly(styrene) particles (diameter  $250\text{--}590\ \mu\text{m}$ ). Removal of the frame from the liquid resulted in the detachment of an air bubble (diameter  $5\text{--}11\ \text{mm}$ ) that was enclosed by a thin liquid film containing a compact monolayer of adsorbed particles (Figure 4B,v). Apart from their gaseous core, gas marbles differ from liquid marbles because of the unique structure of the hybrid (particle-liquid) packaging material (Figure 4B,vi), which comprises two liquid-gas interfaces instead of one (Figure 4B,vii). Liquid in the voids of the particle monolayer results in strong cohesion, because particle displacements out of the monolayer plane are opposed by the attractive capillary forces between neighboring particles (Figure 4B,viii). This balance between compressive stress and surface tension forces is responsible for the exceptional mechanical stability of gas marbles, which can resist both gas removal and

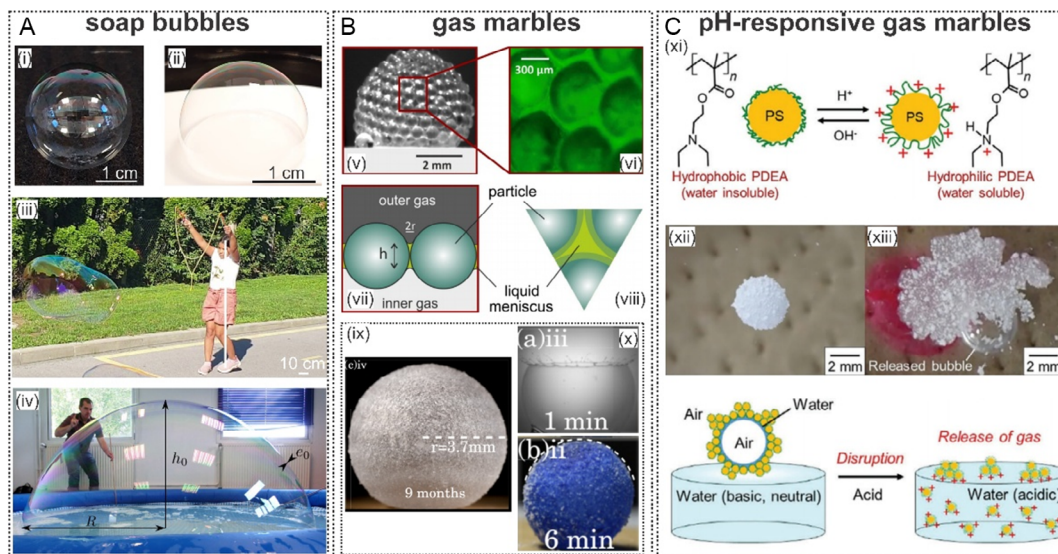


**FIGURE 4** | Examples of packaging strategies for gaseous payloads. (A) The most intuitive gas packaging platform, soap bubbles, in a free-standing (i) and sessile (ii) configuration. Soap bubbles can be made long-lasting by engineering the packaging material composition (e.g., by adding glycerol and/or polymers to surfactant solutions), as exemplified by giant free-standing (iii) and sessile (iv) soap bubbles. Adapted with permission [110]. Copyright 2017, National Academy of Sciences. (B) Gas marbles for packaging gases (v–vi). The packaging material is a film consisting of particles (vii) and liquid (e.g., water), holding particles together by capillary forces (viii). Adapted with permission [60]. Copyright 2017, American Physical Society. By adding glycerol to the packaging material, gas marble lifetime can be prolonged to months (ix) and even years, as opposed to ~1 min and a few min for soap bubbles (x, top) and gas marbles with only water in their shell (x, bottom), respectively. Adapted with permission [111]. Copyright 2022, American Physical Society. (C) Stimuli-responsive gas marbles as responsive gas packaging platforms. By utilizing poly(styrene) microparticles with pH-dependent hydrophobicity (xi), pH-responsive gas marbles are prepared. While such gas marbles float on water for  $\text{pH} \geq 8$  (xii), destabilization followed by payload release occurs for  $\text{pH} < 5$  (xiii). Adapted with permission [39]. Copyright 2024, Wiley.

addition up to applied pressures 10 times the Laplace pressure before collapsing. This concept could lead to new gas packaging processes, supported by the authors' expectation that gas marbles containing up to 0.5% insoluble gas in the encapsulating hybrid film should be stable, showing no significant gas exchange with the surrounding gaseous phase [60, 113].

Roux et al. used polyamide-11 microparticles (diameter  $\sim 160 \mu\text{m}$ ) with intermediate water wettability (contact angle  $71^\circ$ ) to form the packaging material of gas marbles (Figure 4B,ix). Although their presence inhibited gravity-induced liquid drainage, particles alone did not yield long-lasting gas marbles. Typical lifetimes were on the order of minutes, limited by water evaporation (Figure 4B, x, top). Glycerol, able to absorb (desorb) water molecules from (to) the environment and maintain an equilibrium glycerol/water ratio, was added to the aqueous phase to suppress drying. Gas marbles stabilized by the composite water/glycerol/particle film lasted significantly longer than marbles stabilized only by particles, and their lifetime depended on the initial glycerol concentration (Figure 4B, x, bottom). Gas marbles with low initial concentration (glycerol mass fraction  $\leq 0.15$ ) survived for  $\sim 50$  min. Increasing the initial concentration ( $\geq 0.30$ ) led to gas marbles with a lifetime longer than several hours, either by losing water via desorption or gaining water *via* absorption (0.90). Notably, a maximum lifetime of 465 days was reported, with destabilization occurring after this period, attributed to the growth of microorganisms [111].

### 3.4 | Stimuli-Responsive Gas Marbles

Yasui et al. used poly(styrene) microparticles (diameter  $1.58 \mu\text{m}$ ) stabilized with poly[2-(diethylamino)ethyl methacrylate], a pH-

responsive polybase, to demonstrate the first stimuli-responsive gas marble system. At  $\text{pH} \geq 8$ , these polymers are electrostatically neutral and hydrophobic; at  $\text{pH} \leq 6$ , chains become protonated, leading to a hydrophilic polyelectrolyte (Figure 4C,xi). Gas marbles ( $50\text{--}1,000 \mu\text{L}$ ) prepared with these particles and water as the packaging material were robust enough to allow easy handling and manipulation. With water as the only liquid in the packaging material, the gas marble lifetime depended on relative humidity. Wet conditions led to long-lasting gas marbles, as opposed to ambient conditions (lifetimes of  $\sim 70$  and  $\sim 10$  min, respectively). Adding salts or glycerol drastically increased stability, yielding lifetimes of  $\sim$ days and  $\sim$ months, respectively. Gas marbles could also remain stable and be manipulated on planar water surfaces. Thanks to the packaging material responsiveness, gas marble rupture could be controlled by adjusting the pH of the substrate. For  $\text{pH} \geq 8$ , gas marbles retained their structure for  $\sim 1$  h (Figure 4C,xii), whereas gas marbles quickly ( $< 10$  min) disintegrated in acidic conditions (Figure 4C,xiii). Notably, pH-driven payload release was also achieved using a photoacid generator. The capability to control amphibious motion and payload liberation using external stimuli highlights the potential of this system to pack, transport, and release gaseous payloads in a controlled manner. However, scaling up gas marble fabrication remains challenging; automated processes involving robotic systems or (adapted) industrial aeration were suggested as possible solutions [39].

## 4 | Packaging of Solid Payloads

Packaging of solids spans cultural heritage conservation, food preservation, and biomedical applications. Through the selected

examples below, we highlight representative mechanisms and materials, rather than providing an exhaustive survey. We suggest that the readers consider looking into the indicated literature and citations therein [ ].

#### 4.1 | Graphene-Based Packaging Materials

Graphene-based materials offer multifunctional packaging solutions for numerous novel applications due to their exceptional mechanical strength [114], optical transparency [41], conductivity [115, 116], and gas barrier properties [117, 118, 119], leading to preserving delicate artifacts like artworks [40], protecting electronic components [120], and electrochemical enhancement in energy storage applications [121]. Wu et al. packaged silica spheres (diameter 300 nm) via layer-by-layer electrostatic assembly of graphene oxide sheets, resulting in 3D, interconnected graphene oxide shells. Subsequent in-situ magnesiothermic reduction converted the silica spheres into porous silicon while preserving the graphene network (Figure 5A). After thermal treatment ( $\sim 650^\circ\text{C}$  under Ar) and acid etching, porous Si wrapped in graphene was obtained. This two-step strategy demonstrated significant improvements in the electrochemical performance of silicon-based Li-ion battery anodes. This configuration yielded high specific capacities, reaching up to 1100 mAh/g, and enhanced cycle retention compared to non-porous silicon spheres [121]. Note that a conformal graphene shell can simultaneously serve as a mechanical buffer and an electrically conductive, permeable packaging layer.

Yulaev et al. demonstrated self-assembled graphene oxide membranes to immobilize organic and inorganic micro-objects and surfaces for analytical and preservation applications. Dilute aqueous graphene oxide dispersions were drop-cast and dried; graphene oxide segregated at the liquid-liquid, liquid-solid, and liquid-gas interfaces, forming thin, uniform self-assembled membranes around a desired micro-payload (Figure 5B). Slow water evaporation generated a pressure differential of  $10^5$  Pa and compression force of  $\sim 1$  nN between the payload and the packaging material, linked to the shrinkage of the graphene layer. Diverse payloads, including bacteria (*E. coli*), mercury droplets, solid microparticles, and gas bubbles, were immobilized and exhibited controlled shape deformation during shrinkage. Due to transparency to photons and electrons, graphene facilitates high-resolution electron microscopy and Raman spectroscopy [41]. This approach offers an effective barrier against environmental pollutants, UV radiation, and corrosive chemicals [40, 117, 125].

Kotsidi et al. utilized Chemical Vapor Deposition-grown graphene films as 2D protective nanocoatings applied in-situ. Graphene transferred onto a pressure-sensitive adhesive was laminated onto the payload by compression (Figure 5C). This solvent-free approach enabled deposition of single or multiple layers on sensitive surfaces, including artwork and paintings. When more than three layers were used, the protection factor against UV light increased to more than 70%. Interestingly, the coating could be removed with rubber (Figure 5C,ix), without altering the payload appearance (single-layer transparency  $\sim 97.7\%$ ). Spectroscopic analysis revealed that graphene coatings mitigated dye degradation induced by UV and visible radiation, with a reduction of 8% for a single layer, increasing to 25% for

three layers. Through accelerated aging equivalent to 65 years of museum exhibitions, a single graphene layer yielded protection factors of 38% (light blue dye) and 27% (pink dye) [40]. Moreover, defect-free graphene or reduced graphene with multilayers enabled selective permeability of atoms and molecules [118]. By contrast, multilayered graphene or micron-sized sheets exhibited defects, allowing the controlled permeation of gases ( $\text{CO}_2$ ,  $\text{N}_2$ ), ions [117], and small molecules [119]. Graphene has also been employed as an anticorrosion agent in packaging materials [126].

#### 4.2 | Clay-Based Packaging Materials

Two-dimensional clay-based materials have shown promise as multifunctional packaging materials. They are naturally available in various sizes and crystal structures, forming layered structures similar to graphite, such as kaolinite, illite, chlorite, and smectite [123, 127]. These nanolayers regulate gas permeability, microbial activity, and moisture exchange, prolonging fresh produce shelf life without inducing anoxic conditions or accelerated metabolism [28, 63]. The multifunctionality is primarily due to the stacking of nanolayers supported by hydrogen bonds, leading to particles of various sizes (nm to  $\mu\text{m}$ ), with both outer and interlayer functionalities (Figure 5D). These water-dispersible particles bind to numerous nanoparticles, foreign molecules, and drugs, making them an efficient packaging material [64, 128]. For example, gas bubbles dispersed in an aqueous suspension of clay nanoplatelets aggregate into a thin, microporous layer, resulting in stable armored bubbles and porous vesicles [129].

Eguchi et al. used films made from saponite clay ( $\sim 20$ – $50$  nm platelets;  $\sim 20$   $\mu\text{m}$  film thickness) to package fruits [62]. When applied onto apples and bananas, oxygen permeability was reduced by 146 times compared with commercially used poly(vinylidene chloride) films. Smaller platelets enhanced adhesion and uniformity (Figure 5D,x), thereby reducing gas permeation and respiration. Larger montmorillonite platelets (100–1000 nm) reduced porosity by efficient packing, hence further suppressing  $\text{O}_2$  diffusion. Gas permeation (driven by diffusion) was due to capillary action on the film. When the film comprised small particles that adsorbed water molecules, oxygen permeation could be controlled by adjusting the humidity. Contrarily, films composed of larger particles showed reduced gas permeation, attributed to fewer pores in the film due to efficient packing. Such a reduction in gas exchange from fresh produce, promoted lower production of spoilage-related volatile compounds from metabolic processes (e.g., alcohols, aldehydes, esters), thereby extending freshness for up to 4 months, depending on the fruit payload (Figure 5D,xi) [63].

The mechanical strengthening of low-density poly(ethylene) using a clay/ $\text{TiO}_2$  nanocomposite also significantly enhances its mechanical properties and barrier performance. Bodaghi et al., prepared melt-blended films containing 3 wt.% clay (Cloisite 20A) and/or 3 wt.%  $\text{TiO}_2$ , along with 0.5 wt.% glycerol, with a thickness of 30  $\mu\text{m}$ . The Young's modulus increased from 89 MPa to 141 MPa, while the tensile strength rose from 10.4 MPa to 12.8 MPa; at the same time, oxygen permeability decreased by  $\sim 51\%$ , and  $\text{CO}_2$  permeability decreased by  $\sim 32\%$  compared with the pure polymer. These barrier performance gains correlated

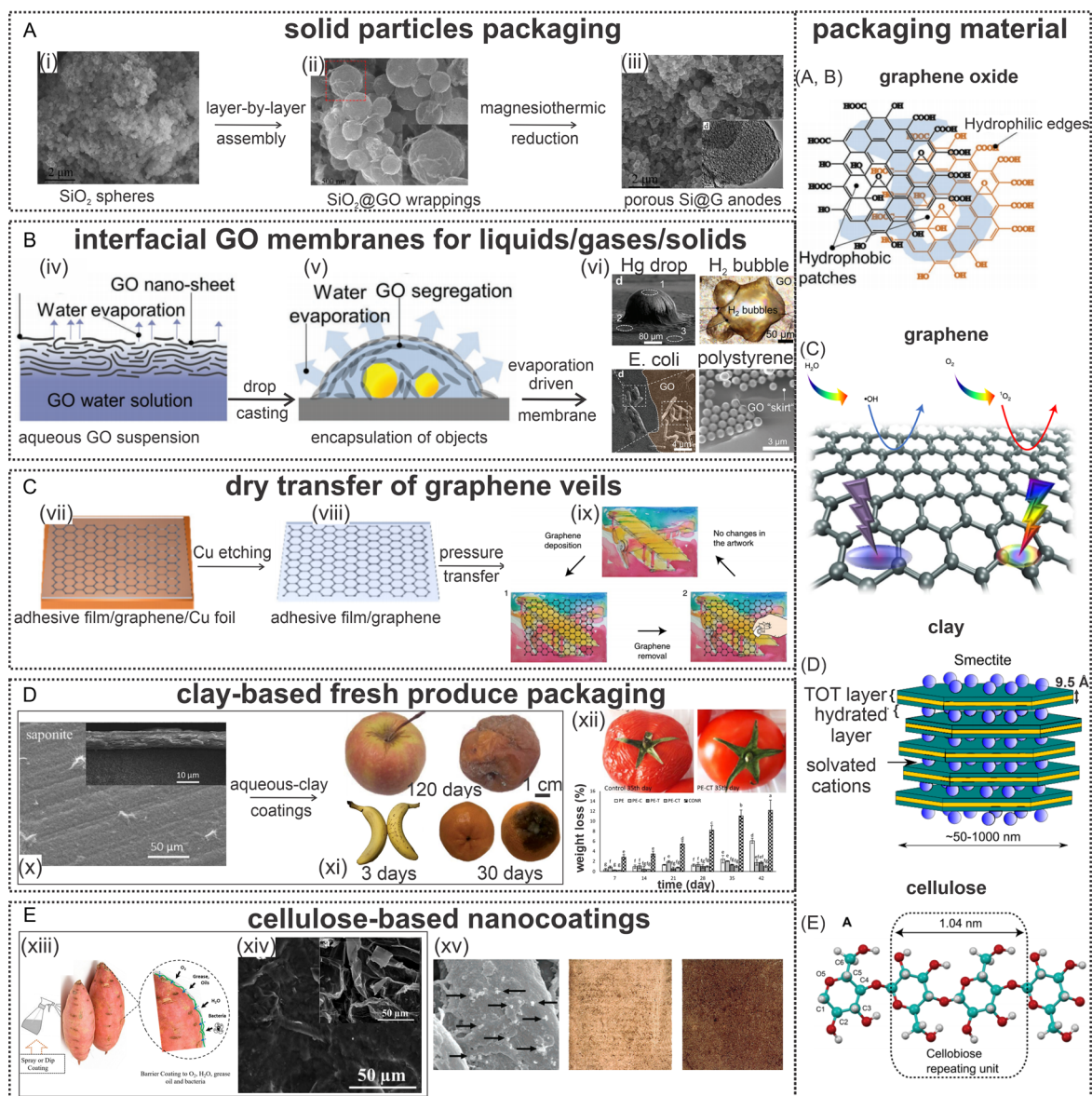


**FIGURE 5** | Examples of packaging strategies for solid payloads. (A) Layer-by-layer electrostatic assembly of graphene oxide (GO) produces a 3D network of graphene-wrapped porous silica spheres, serving as a precursor for in-situ magnesiothermic reduction. Electron microscopy images of (i) silica spheres, (ii) silica spheres embedded in graphene oxide, and (iii) porous silica embedded in GO. Adapted with permission [121] copyright 2014 American Chemical Society. (B) Evaporation-driven self-assembly of drop-cast aqueous GO forms continuous, conformal, electron- and optically transparent membranes that enclose diverse microobjects. (iv) Interfacial segregation, (v) encapsulation/membrane formation, and (vi) Hg microdroplet, H<sub>2</sub> bubbles, poly(styrene) beads, and *E. coli*, as payloads of different sizes. Adapted with permission [41]. Copyright 2016, Wiley. (C) Solvent-free transfer of graphene veils for artwork preservation. Monolayer graphene grown on Cu is laminated to a pressure-sensitive adhesive, Cu is etched, and the veil is pressure-transferred at 0.1–0.5 MPa (50°C–55°C). (vii) graphene/pressure sensitive adhesive on Cu, (viii) after Cu etch, (ix) transfer and removal with an eraser. Adapted with permission [40]. Copyright 2021, Springer Nature Limited. (D) Air-dried saponite coatings form ~20 μm thick inorganic barriers on fresh produce. (x) SEM images of the top surface and cross-section of the film (left), and photographs of clay-packaged fruits (right) versus fruits wrapped with poly(ethylene) films (control experiment, (xi)). The mold on oranges and apples and the sugar spots on bananas, are observed at different times, indicating the effective blocking of less-polar volatiles and thus the enhanced protection offered by the clay coating. Adapted with permission [62]. Copyright 2022, CC BY 4.0, Royal Society of Chemistry. (xii) Low-density poly(ethylene) nanocomposite films (containing clay and TiO<sub>2</sub>) minimize tomato weight loss. Adapted with permission [122]. Copyright 2024, CC BY 4.0, BMC Plant Biology. (D) The clay schematic picture, adapted with permission [123]. Copyright 2020 The Eur. Phys. J Special Topics. (E) cellulose-based nanocoatings. (xiii) Hand-held spray biocoatings (cellulose nanofibers + pectin + phenolic extract, with essential oil and glycerol) form protective films on sweet-potato surfaces, (xiv) SEM of a CNF:pectin:phenolic ratio 2.5:1.25:1, respectively (inset: uncoated control). Reproduced with permission [66]. Copyright 2025, CC BY-NC-ND 4.0, Elsevier. (xv) SEM image of Ca(OH)<sub>2</sub> nanoparticles on cellulose fibers and 19th-century paper specimens (deacidified vs. untreated) after identical artificial aging. Brown color represents degradation. Adapted with permission [65]. Copyright 2002, American Chemical Society. The cellulose chemical structure is adapted with permission [124]. Copyright 2022, CC BY-NC 4.0, American Association for the Advancement of Science.

with reduced fungal activity and lower ethylene production, allowing tomato preservation for up to 42 days at 4°C (Figure 5D,xii) [122]. By using a mixture of sillimanite and bentonite clays (~80–110 nm sizes), Kumar *et al.* reported enhanced ethylene scavenging under ambient conditions. Ethylene removal reached 84% over 21 days, depending on temperature and relative humidity (best at 29°C and 55%, respectively), thereby extending the shelf life of fresh fruits at 29°C [28].

### 4.3 | Starch and Cellulose-Based Packaging Materials

Cellulose, the most abundant biopolymer, and starch, a plant-derived polysaccharide, are critical for developing bioderived packaging materials due to their sustainability and biodegradability [21, 29, 130, 131, 132]. Their derivatives can be processed into continuous films, coatings, or fibrous mats. However, these biopolymers often suffer from brittleness and sensitivity to water, necessitating reinforcement with cellulose nanofibers or nanocrystals to enhance their mechanical and barrier properties [133]. The tensile strength of these cellulose-based nanomaterials reaches ~150 MPa, with an elastic modulus ~15 GPa in film form, making them strong for use in packaging compared to many petroleum-based plastics [134]. Moreover, the rod-like shape of cellulose nanomaterials promotes cholesteric self-assembly, enabling the formation of dense, transparent coatings via layer-by-layer or casting routes [66, 135–137].

The strong hydrophilic nature of cellulose and its anisotropic interactions with water [124, 138] pose significant challenges, particularly in maintaining water and oxygen barrier properties under humid environments (RH > 50%) [139, 140], essential for many packaging applications [133]. To overcome this, hybridization techniques (e.g., incorporating inorganic nanoparticles, polymers, or other fillers) have been investigated for further enhancing mechanical strength, moisture resistance, and barrier efficiency [134, 141, 142]. For instance, cellulose nanowhiskers, isolated via acid hydrolysis into rod-like nanoscale crystals, have been used to form dense, percolating networks that improve structural integrity and resistance to gas and water vapor transmission [130]. Importantly, pH-sensitive dyes extracted from plants [143] can be mixed with packaging materials, thus allowing the packaging film to sense the payload freshness through visual inspection of its color [144, 145].

In the context of active and intelligent packaging, Zhou *et al.* developed double-layer indicator films comprising konjac glucomannan/camellia oil and  $\kappa$ -carrageenan loaded with pH-sensitive dyes like curcumin and anthocyanins. These packaging materials showed improved moisture resistance and mechanical strength. Furthermore, their responsiveness to pH changes due to payload spoilage with color changes, enabled their use for real-time monitoring of meat freshness [146]. Similarly, Wu *et al.* reported a shrimp freshness visual indicator based on gellan-gum films incorporating *Clitoria ternatea* extract, combined with heat-treated soy protein. This composite packaging material provided controlled release of anthocyanins, antioxidant activity, and antibacterial effects, and acted as pH indicator showing color changes from violet to yellow for pH values from 1 to 14 [29]. Moreover, cellulose acetate/cellulose nanofiber composite films containing anthocyanins exhibit color changes upon exposure to

ammonia released by degrading meat and fish, illustrating how nanocellulose improves dye uptake and sensing performance in practical packaging geometries [147].

Very recently, Abouzeid *et al.* formulated sprayable nanocoatings from cellulose nanofibers blended with pectin and phenolic extracts derived from sweet potato peel. Glycerol and essential oil were also used to tune the formulation rheological parameters (Figure 5E). When applied to sweet potato roots, these coatings reduced respiration rate by up to 72% and decreased weight loss by ~51%, compared with uncoated roots, while remaining optically clear and uniform. Additionally, the same anthocyanin extracts provided pH-responsive color (red at pH < 5 to blue-purple at pH > 9), serving as components of smart packaging materials able to detect antioxidants and act as freshness indicators [66]. Complementarily, Souza *et al.* used nanocellulose-stabilized Pickering emulsions of plant essential oils to cast thermoplastic-starch films. Emulsions containing 2–5 wt.% essential oils (e.g., camphorwood, cinnamon, cardamom) were cast on poly(styrene) plates along with 4 wt.% starch. These films exhibited stronger polymer–emulsion interactions and thus enhanced mechanical resistance and reduced water vapor transmission, highlighting their potential for biodegradable active packaging [148].

Beyond food applications, cellulose aging and deacidification remain central for long-term preservation of payloads. The aging of cellulose is primarily driven by the depolymerization of cellulose fibers under acidic conditions. Numerous efforts are being made to strengthen cellulose by applying deacidification conditions using micro- and nanoparticles [149, 150]. Giorgi *et al.* spray-coated 19th-century paper specimens with calcium hydroxide particles (260 nm) dispersed in propanol, achieving deacidification via carbonation, thus prolonging the degradation window [65] (Figure 5E,xv). Wu *et al.* deposited a NaOH/urea bacterial cellulose solution onto an acidic state of paper through ultrasonic atomization for strengthening the paper [151]. Finally, Reynaud *et al.* demonstrated the presence of ~5,000 years old cellulosic textiles in archaeological sites, with this long lifetime attributed to mineral-induced preservation mechanisms. Such an in-place molecular preservation (silicification) is supported by aqueous transport of inorganic compounds (metal cations and soil solutes) onto cellulosic textiles, where nanoscale mineral deposition stabilized cellulose against microorganisms and fungi [152]. These findings suggest the potential of exploring these mineral-assisted stabilization routes for future cellulose-based packaging.

### 4.4 | Nanocomposite Packaging Materials

Hybrid polymer–inorganic nanocomposites are powerful packaging materials for enclosing and releasing particulate payloads with tunable structure and kinetics [153, 154]. Using microfluidics, Udoh *et al.* emulsified aqueous mixtures of sodium poly(styrene sulfonate) (1–5 wt.%) and silica nanoparticles (22 nm) into hexadecane at a flow-focusing junction. Nucleation and growth of polymer-silica composite droplets, using ethyl acetate as the extraction solvent at high Péclet numbers, resulted in droplet solidification into capsules with isotropic and anisotropic shapes and internal morphologies from nucleated to bicontinuous structures. Upon immersion in water, the capsules exhibited

directional, pulsed release of micrometer-scale nanoparticle clusters. The release profile and timescale could be tuned (e.g., by adjusting the pH). At the same time, the scaffold remained largely intact, demonstrating a nanocomposite packaging route for solid payloads with programmable dissolution behavior [155].

## 5 | Packaging of Payloads of Various Phases

A single packaging strategy can address payloads comprising more than one phase (e.g., liquid foam consisting of gas bubbles dispersed in a liquid phase [106] or cell cultures comprising cells in an aqueous medium [45]) or various payloads across different physical states. Below, we discuss representative examples of both.

### 5.1 | Foam Marbles

Submicrometer particles (and their aggregates) can simultaneously stabilize a macroscopic aqueous drop and microscopic bubbles dispersed in the aqueous phase. The resulting object is a foam marble, a liquid marble with a particle-stabilized foam core (Figure 6A,i). To prepare foam marbles, Aono et al. used poly(styrene) particles (diameter ~410 nm) stabilized with poly(N, N-diethylaminoethyl methacrylate) chains. An aqueous particle dispersion at pH 10 was first mixed with air to form a particle-stabilized foam of polydisperse bubbles (diameters ~70–880  $\mu\text{m}$ ; Figure 6A,ii). Then a drop of this foam was rolled onto a dry bed of the same particles, resulting in ~5 mm foam marbles (Figure 6A,iii). This air–water–air dispersed structure featured dry particles adsorbed at the foam drop surface as ~20  $\mu\text{m}$  large aggregates. Air pockets trapped within this rough aggregate-based coating generated a hierarchical roughness and high liquid repellence, despite the intrinsically hydrophilic primary nanoparticles. This behavior was consistent with a metastable Cassie–Baxter wetting state. In contrast, particles adsorbed at the bubble air–water interface, responsible for stabilizing the foam, were described by a Wenzel-type wetting state. Foam marbles were easy to manipulate (Figure 6A,iv) and, upon drying, retained a porous internal structure (Figure 6A,v). These features make them attractive as soft, multicomponent packaging platforms for handling gas payloads or as porous materials for cosmetics, food manufacturing, and personal care formulations [67].

### 5.2 | Capillary Containers

Zhang et al. introduced “capillary containers,” a packaging concept based on 3D fluid interfaces that could be manipulated in a programmable manner using external fields. Capillary containers were fabricated by attaching steel microbeads (diameter 500  $\mu\text{m}$ ) onto the vertices of 3D-printed resin polyhedral frames (Figure 6B,vi). Permanent magnets mounted on a motorized translation stage were used for contactless magnetic manipulation. By engineering the wettability of the capillary container, one fluid (fluid 1) could be trapped in another immiscible fluid (fluid 2). The authors demonstrated water payloads (fluid 1) in air (fluid 2), air in water, water in oil, oil in water, ethylene glycol in air, air in ethylene glycol, ethylene glycol in oil, and oil in ethylene glycol (Figure 6B,vii–x). Container sizes (~1.2–4.6 mm) were tuned to package liquid payloads of various volumes (Figure 6B,xi). By varying the frame geometry, liquid packages with complex

shapes were produced, such as pyramids, prisms, various polyhedra, and buckyballs (Figure 6B,xii) [68]. Beyond shape and phase diversity, capillary containers also exhibited rich dynamic functionalities (e.g., field-directed transport and controllable release), which are discussed in more detail in Section 6.3.

## 5.3 | Water-Templated Superglue Films

Jampani et al. developed WRAPPINGS (Water-based, Room temperature, Atmospheric Pressure Polymerization of INSTANT Glues controlled by Surfactants), which uses water-templated interfacial polymerization of cyanoacrylate to generate poly(cyanoacrylate) films on liquid interfaces. WRAPPINGS relies only on water, a surfactant, and a cyanoacrylate monomer, and poly(cyanoacrylates) are biocompatible and biodegradable; this provides an eco-friendly route to prepare thin polymer films with precisely engineered microscopic and macroscopic properties. In a typical process, the free surface of an aqueous phase containing cationic surfactants is exposed to cyanoacrylate vapor (Figure 6C,xiii). Interfacial OH<sup>-</sup> groups initiate anionic polymerization, resulting in long poly(cyanoacrylate) chains confined to the interface. Electrostatic attraction between the surfactant head group and the oppositely charged active poly(cyanoacrylate) chain modulates growth rate. The surfactant-decorated water surface templates polymerization, and polymer chains aggregate into a continuous film covering the entire free surface. This strategy packages liquid, gas, and solid payloads.

Liquid of various forms, volumes, and compositions were packaged with WRAPPINGS. This included sessile drops (~few  $\mu\text{L}$  to ~100  $\mu\text{L}$ ) and puddles (~200  $\mu\text{L}$ ) on solid substrates (Figure 6C,xiv), and larger aqueous volumes (~7.5 mL) in dishes, where the polymer film served as a sealing cap (Figure 6C,xv). Application to pendant drops (~10  $\mu\text{L}$ ) yielded self-standing, dumpling-shaped liquid packages (Figure 6C,xvi). Payloads ranged from aqueous solutions of surfactants, polyelectrolytes, amino acids, salts, indicators, and dyes to samples containing living microorganisms (*Daphnia*). WRAPPINGS also shows promise for packaging solid payloads: partial conformal polymer coatings on solids of arbitrary shapes (Figure 6C,xvii) suggest that these films could similarly wrap various other objects. Finally, sessile and free-standing soap bubbles made from cationic surfactant solutions (Figure 6C,xviii) were used as templates to package and manipulate gas payloads. Here, the liquid film enclosing a few to tens of mL of gas served as the polymerization template, resulting in elastic poly(cyanoacrylate) films around gases such as air, CO<sub>2</sub>, or air mixed with acetic acid or triethylamine (Figure 6C,xix–xx) [24].

## 6 | Multifunctional and Responsive Packaging

### 6.1 | Edible Liquid and Gas Marbles

Kawamura et al. noted that liquid marbles based on edible, low-toxicity particles (as opposed to, e.g., poly(tetrafluoroethylene)) could be utilized as platforms for preparing food products or oral formulations for health care applications. They were the first to enclose aqueous liquids using edible lipid crystals (Figure 7A, i). In a typical experiment, a water drop (5  $\mu\text{L}$ ) was rolled sequentially over coarse (~355–500  $\mu\text{m}$ ) and then finer (<180  $\mu\text{m}$ ) lipid

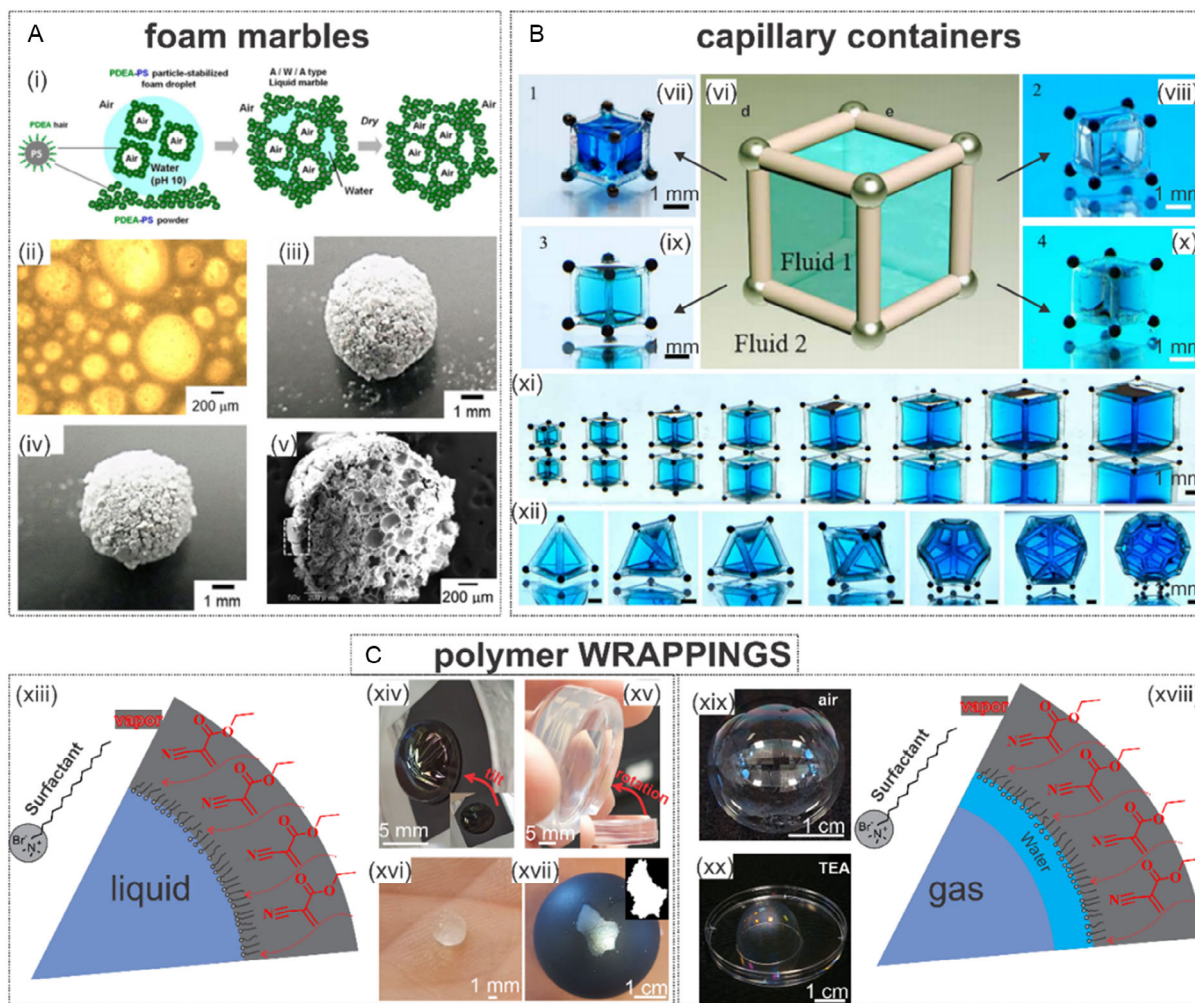


**FIGURE 6** | Examples of packaging strategies for payloads of various phases. (A) Foam marbles: a particle-stabilized aqueous foam serves as the multiphase core, and the packaging material also consists of particles (i). Poly(styrene) nanoparticles functionalized with poly(*N*, *N*-diethylaminoethyl methacrylate) stabilize both the microbubbles in the foam (ii) and the macroscopic foam drop (iii). Drying the foam marble (iv) and imaging its cross-section (v) reveal a porous internal structure. Adapted with permission [67]. Copyright 2022, American Chemical Society. (B) Capillary containers as a packaging strategy for enclosing payloads of various phases with a metallic packaging material (vi). Various fluid pairs can be packaged, such as water in air (vii), air in water (viii), water in oil (ix), or oil in water (x). This strategy allows control over payload volume (xi) and shape (xii), including polyhedral and buckyball-like containers. Adapted under the terms of the CC BY license [68]. Copyright 2021, Science Publishing Group. (C) WRAPPINGS: in-situ packaging of fluid or solid payloads with polymer films formed by interfacial polymerization of cyanoacrylate monomers at surfactant-decorated water interfaces. Applied to aqueous solutions (xiii), WRAPPINGS yields aqueous packages such as puddles supported by a solid substrate (xiv), large volumes sealed in containers (xv), and self-standing liquid dumplings (xvi). The partial coating of a table tennis ball shows the potential for packaging solid payloads of arbitrary shape (xvii). When applied to soap bubbles (xviii), WRAPPINGS produces solid membranes that package inert (air, CO<sub>2</sub>) or reactive (triethylamine) gaseous payloads (xix–xx). Adapted under the terms of the CC BY license [24]. Copyright 2024, Wiley.

crystal particles, resulting in a liquid marble (Figure 7A,ii). Heating close to the melting point of the lipid crystal converted the marble into a capsule (Figure 7A,iii). The study of liquid marbles prepared with different lipids (i.e., fatty acids and triglycerides) showed that the marble lifetime on a solid surface increased with the alkyl chain length of lipids, attributed to the lower water solubility of long alkyl chain lipids. The mechanical robustness of stable liquid marbles was retained after transforming them into capsules. Furthermore, liquid marbles (but not capsules) stabilized with lipids having an alkyl chain with more than 16 carbon atoms could float on water. Interestingly, fatty acid-stabilized liquid marbles were pH-responsive: lower pH extended the marble lifetime on water, whereas the stability of triglyceride-coated liquid marbles was pH-independent [48].

Very recently, Mame-Khady et al. demonstrated that macroscopic edible particles can package non-aqueous liquids used in the food industry. Commercial silver dragées, sugar spheres (diameter ~1.9 mm) coated with a sub- $\mu\text{m}$  silver layer, were hydrophobized with edible stearic acid and used to stabilize poly(glycerin) drops (~30–100  $\mu\text{L}$ ), forming liquid marbles. Notably, aqueous liquid marbles could not be formed because the silver dragées dissolved in water. Application of mechanical stress and/or merging led to interfacial jamming of the particles; the resulting plastic deformation of the particle-laden fluid interface enabled the creation of non-equilibrium liquid marble shapes, such as letters. The same particles could encapsulate other edible liquids (e.g., poly(glycerol monolaurate), a plant-based surfactant), highlighting the potential use of this packaging method

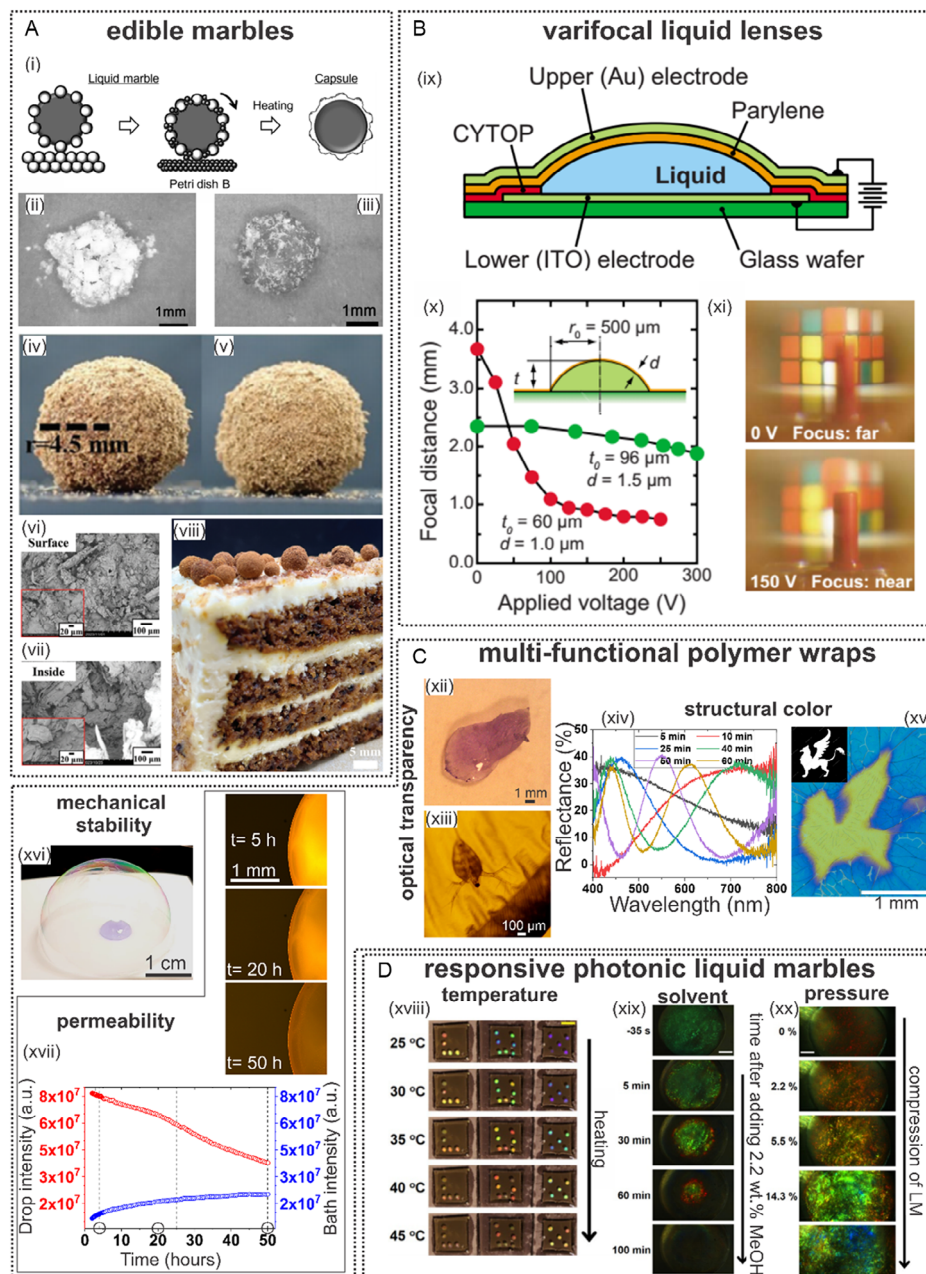


**FIGURE 7** | Examples of multi-functional and responsive packaging strategies applied to various payloads. (A) Packaging of liquid and gas payloads with an edible packaging material. A water drop is coated with lipid crystal particles of two different sizes (i). The resulting liquid marble (ii) is transformed into a capsule (iii) by melting the lipid crystals. Adapted with permission [48]. Copyright 2012, Japan Oil Chemists' Society. Cinnamon, comprising irregularly shaped microparticles, as the key component (along with water) of the packaging material of an edible gas marble (iv). The marble remains mechanically stable even after water evaporation (v), thanks to the stabilizing layer of jammed cinnamon particles at the air-water interface (vi-vii). Other edible liquids can be components of the packaging material, leading to gas marbles of interest for molecular gastronomy applications (viii). Adapted with permission [61]. Copyright 2025, Wiley. (B) Varifocal lens based on a liquid payload enclosed with an electrically responsive polymeric packaging material. A low vapor pressure liquid drop on an electrode substrate is packaged with a thin poly(p-xylylene) film, and a nanometric Au layer is deposited onto the film (ix). Upon application of voltage, the shape of the packaged drop is modulated, leading to a controlled variation in the focal length of the liquid lens (x), as shown by the change of focus (xi). Adapted with permission [50]. Copyright 2008, American Institute of Physics. (C) Multi-functional packaging of various payloads via the in-situ growth of thin poly(cyanoacrylate) films onto payloads. The transparency of the packaging material is exploited for real-time observations within liquid packages, such as the occurrence of a chemical reaction (xii), or the movement of living organisms (*Daphnia*, (xiii)). The precisely controlled film thickness offers a packaging material with on-demand structural color, as demonstrated with films having a single color (xiv) or films with two-color patterns (xv). Soap bubbles, containing a payload consisting of a liquid specimen surrounded by air, when polymerized, yield a mechanically stable and optically clear reaction chamber (xvi). Slow dye release from a polymer-packaged solution drop (payload) into a liquid environment (xvii). Adapted under the terms of the CC BY license [24]. Copyright 2024, Wiley. (D) Packaged complex fluid payloads serving as sensors for external perturbations via a photonic response. Enclosing a cholesteric liquid crystalline solution of hydroxypropylcellulose with fumed silica nanoparticles leads to liquid marbles with structural coloration. Changes in temperature (xviii), exposure to chemicals (xix), or mechanical compression (xx) are sensed through color variations detectable by eye. The scale bars are 5 mm (xviii) and 500  $\mu\text{m}$  (xix-xx). Adapted under the terms of the CC NC license [35]. Copyright 2020, Wiley.

in molecular gastronomy applications. The macroscopic size of these liquid marbles makes them visible to the naked eye, and their texture contributes to sensorial perception of the package. These important features were demonstrated by a honey liquid marble, used as an edible decorative element on a cake [156].

Mukai et al. showed that cinnamon can act as a robust edible packaging material for producing ultra-stable gas marbles. These macroscopic air payloads were packaged in an air environment using a hybrid packaging material comprising irregularly shaped cinnamon particles (needle-like, average diameter  $\sim 160 \mu\text{m}$ ) and various edible liquids. Note that hydrophilic cinnamon particles were used as received, thus eliminating the constraint of chemical treatment typically required for hydrophilic particles. To produce a gas marble, the authors first prepared a thick particle raft by depositing dried cinnamon on water. Quickly after this step (i.e., before the cinnamon particles were wetted by water), an air bubble was injected below the air-water interface and was manually moved around to promote spontaneous particle adsorption at the bubble surface, resulting in gas marbles with diameters 2.4–7.2 mm (5–200  $\mu\text{L}$ ) (Figure 7A,iv). Cinnamon-stabilized gas marbles remained intact after being transferred onto hydrophilic glass or when moved by air blowing. Remarkably, even after complete evaporation of the liquid component, the dried gas marble could maintain its 3D structure for more than a year (Figure 7A,v). Heating or cooling ( $-25^\circ\text{C}$ – $150^\circ\text{C}$ ) of these stable gas marbles did not disrupt the shell structure. This exceptional mechanical stability was attributed to the thick layer of jammed particles at the gas marble surface (Figure 7A,vi–vii). This network of interlocked particles was further reinforced during drying because mechanical compaction led to an increased packing density. Gas marbles incorporating various edible liquids (milk, coffee, vinegar, soy sauce) in their shell were used to decorate hot dishes and desserts (such as meat or cake (Figure 7A,viii)) [157].

## 6.2 | Liquid Packages With Optical/Photonic Functionality

Binh–Khiem et al. used drops packaged by polymer films as liquid lenses with electrically tunable focal length. The main element of the lens was a sessile drop of non-volatile liquid (glycerin, liquid paraffin, silicon oil) sitting on glass with a patterned indium tin oxide (bottom electrode). The drop was enclosed with a thin poly(p-xylylene) film, created by chemical vapor deposition at room temperature under vacuum. The film thickness could be varied from 0.1 to  $\sim 1 \mu\text{m}$ , and the low surface roughness ( $\sim 2 \text{ nm}$ ) ensured high optical quality. Packaged liquid drops could be up to 30 mm in diameter, much larger than the capillary length. Furthermore, a 5 nm-thick Au layer was deposited onto the polymer, serving as the top electrode (Figure 7B,ix). When voltage was applied, electrostatic attraction between the electrodes competed with the elastic response of the film, dictating the shape of the liquid lens, which in turn determined the focal distance (Figure 7B,x–xi). The application of 150 V on a liquid lens with 1 mm diameter and  $60 \mu\text{m}$  height resulted in 20% reduction in the (initial) focal length; shape changes were repeatable and reversible. The fabrication of single liquid lenses with microscopic to macroscopic sizes (diameter  $20 \mu\text{m}$ –30 mm), as well as lens arrays has been shown [50].

At a much larger length scale, packaging of nonvolatile liquids with thin metallic layers has been explored as the basis for a Lunar Liquid Mirror Telescope, an instrument that could be potentially installed on the Moon. This groundbreaking concept combines the absence of mechanical parts with significantly lower mass (i.e., lower shipping costs), compared to glass-based telescopes. Two key requirements for the liquid are low vapor pressure and low freezing temperature, so that the material does not evaporate in high vacuum and remains liquid under very low temperatures. To meet these needs, Borra et al. used the ionic liquid 1-ethyl-3-methylimidazolium ethylsulfate as the core liquid-payload. Metallic films used as a packaging material were deposited under vacuum to impart high reflectivity. First, silver was directly deposited onto the ionic liquid, which led to reflective films comprising Ag nanoparticles (diameter  $\sim$  a few tens of nm), resulting in infrared reflectivity ( $> 60\%$ ). However, the tendency of Ag diffusion into the ionic liquid limited the ability to obtain thick-film coatings. To overcome this, the authors initially deposited a Cr film (5 nm thickness) onto the ionic liquid before depositing an additional Ag layer (30 nm thick). The infrared reflectivity of the liquid enclosed with this compound metal packaging material was significantly improved compared to the Ag-coated ionic liquid. The combination of high optical quality, reflectivity, and environmental robustness of metal-coated ionic liquid highlighted the potential of this packaging strategy [55].

## 6.3 | Other Multifunctional Packages

Capillary containers (Figure 6B) offer another route to multifunctional packaging, where payload handling is coupled to controlled release. Zhang et al. showed that such containers, assembled from magnetically responsive microbeads, exhibit multiple modes of motion (e.g., flipping, rotation, translation). The motion could be tuned by adjusting the distribution of the microbeads and the motion of the applied magnetic field. These dynamic responses were exploited to demonstrate selective operations with sample fluids at various (immiscible) fluid environments. For instance, utilizing the appropriate surface modification, a capillary container could pick up gas bubbles in water or collect water droplets in oil. Such responsive packaging material was used to show different chemical reactions, such as the catalytic decomposition of  $\text{H}_2\text{O}_2$  in oil, an organic (addition) reaction in oil, and a multistep reaction (powder dissolution in a solvent, precipitation, and transport of products -as reactants- between steps). A capillary container was also used to package an aqueous  $\text{CaCl}_2$  solution in a sodium alginate bath. Interfacial gelation driven by physical crosslinking of the alginate chains by the  $\text{Ca}^{2+}$  ions, yielded a porous membrane shell enclosing the core liquid. To investigate the potential of this core-shell structure in drug delivery and release applications, the authors first dissolved riboflavin in the  $\text{CaCl}_2$  solution, which was then packaged as described above. The dynamic release of riboflavin into a water bath was studied under different pH conditions [68].

## 6.4 | Packaging of Living Cells

The packaging of complex fluid payloads comprising cells and their culture medium is a topic of broad interest, from

fundamental understanding of cell dynamics to tissue engineering, with many scientists focusing on repairing or replacing damaged organs. Several approaches have been implemented to achieve this goal. For example, cell arrangements and the formation of topological structures on functional planar polymer surfaces [158, 159], hydrogels [160], shape-memory scaffolds [161], and many other systems [27] have been investigated. In all cases, the packaging material must act as a replacement for the extracellular matrix; thus, the enclosed cells (payload) have access to nutrient flow, native growth and proliferation conditions, gas flow, waste excretion, and appropriate mechanical and biochemical cues.

Tan et al. utilized a microfluidics approach to package cancer and yeast cells in lipid vesicles. Cells were emulsified in a liquid lipid phase consisting of phospholipids and oleic acid, before exposure to an aqueous ethanol solution. Ethanol extracted in water promoted the removal of oleic acid and drove insoluble phospholipids (both ethanol-soluble and -insoluble phospholipids) to reassemble into stable giant vesicles. This solvent-free process produced cell-laden vesicles within minutes, maintained cell payload viability, and allowed for limited ion exchange, with vesicle stability exceeding 26 days [162]. Similarly, He *et al.* used a T-junction microfluidic channel coupled with optical trapping to selectively encapsulate a single cell or even mitochondria into pL to fL aqueous droplets. A nanosecond-pulse laser was used to rapidly induce cell photolysis, supporting single-cell enzymatic assays, which illustrated how packaging living-cell payloads at small volumes facilitates precise measurements at the single-cell level [163]. As a matrix-based alternative, Utech et al. produced highly monodisperse, structurally homogeneous alginate microgels by separating droplet formation from gelation. Here, droplet microfluidics generated aqueous droplets containing alginate and a water-soluble calcium-ethylenediaminetetraacetic acid complex in the oil phase. Later, Ca<sup>2+</sup> ions were released by adding acetic acid to the oil, promoting uniform crosslinking of alginate. Single mesenchymal stem cells encapsulated in these microgels remained viable, with cell growth and proliferation monitored over a 2-week period, providing a controllable 3D microenvironment with continuous access to nutrients [164]. Lastly, even more complex microfluidic designs have been used to package and sort cells using piezoelectric elements within the channels [165].

The WRAPPINGS method is a prominent packaging strategy that combines straightforward implementation with precisely controllable packaging materials, providing additional functionalities (Figure 7C). Thin poly(cyanoacrylate) films grown from monomer vapors exhibit high uniformity (<2% thickness variation over 1 cm<sup>2</sup> area) and low roughness (~4 nm), leading to transparent coatings allowing observation of the enclosed payload with the naked eye (see chemical payload in Figure 7C,xii) or via microscopy (biological payload, Figure 7C,xiii). A well-defined growth rate of ~8 nm/min permits an accurate control of the thickness of the packaging film by adjusting the reaction time. Tailoring this microscopic property, in turn, leads to tailored macroscopic properties. For example, modulating the thickness leads to films with a single, uniform interference color that is tunable (Figure 7C,xiv) or complex color patterns (Figure 7C,xv). The mechanical properties of films can also be tuned. For example, a liquid dumpling is formed when a sessile drop is enclosed by a poly(ethyl cyanoacrylate) shell with a

Young's modulus high enough for handling the liquid payload with tweezers. At the same time, the polymer film is sensitive enough to mechanical stress, allowing film breaking and merging of the dumplings; this allows ingredients to mix and realize a chemical reaction (Figure 7C,xii). This is a demonstration of on-demand reaction chambers, prepared in a Do-It-Yourself fashion (Figure 7C,xvi). Permeability can also be engineered by adjusting thickness: A sufficiently thick poly(butyl cyanoacrylate) film enclosing a drop of aqueous dye solution could keep the drop intact upon water immersion, whereas thinner films enabled dye release over days [24].

Anyfantakis et al. demonstrated another multifunctional package by enclosing a mechanochromic material inside liquid marbles. Liquid marbles were used here as miniature platforms to drive the self-organization of hydroxypropylcellulose into a cholesteric liquid-crystalline phase with a programmable structural color. The optical periodicity (cholesteric pitch) of the structure is the distance along the helix required for the liquid crystal director to make a complete 360° rotation, which defines Bragg's reflection window (birefringence \* pitch). Drops of aqueous hydroxypropylcellulose solution, with a polymer concentration in a regime where an isotropic and a cholesteric phase coexist, were rolled onto hydrophobic silica nanoparticles. Here, the role of nanoscale particles was also to reduce light scattering, ensuring a transparent marble. Controlled water extraction into a known volume of dry organic solvent increased the polymer concentration to within the cholesteric regime, yielding marbles with macroscopically homogeneous structural color. The hydroxypropylcellulose concentration set the Bragg reflection photonic bandgap. Interestingly, these complex fluid payloads behaved as millimetric soft sensors that responded to different external stimuli with visible color changes to the naked eye, in real time. Heating induced a red shift and cooling a blue shift in the reflected color (Figure 7D,xviii), and mechanical compression caused a blue shift (Figure 7D, xx). These responsive liquid payload packages also could detect methanol in their environment by exhibiting a blue shift (Figure 7D, xix) [35].

## 6.5 | Toward Functional Packaging at Large Scales

Functional packaging concepts can, in principle, be extended far beyond the microscale; for instance, they may address challenges at architectural and infrastructural scales. An interesting example is the concept of enclosing (either in part or entirely) buildings with a packaging material that provides, in real time, information about their structural health. Čamo et al. explored mechanochromic coatings based on cholesteric liquid crystal elastomers for structural health monitoring of buildings. They formulated a liquid coating that could be directly painted onto construction materials and converted into a cholesteric liquid crystal elastomer via self-assembly combined with photopolymerization. The resulting elastic/rubbery coating served as a mechanochromic strain sensor that responded to strain by changes in structural color arising from the periodic internal cholesteric structure, analogous to the photonic response of cholesteric liquid marbles [35]. When applied to extruded poly(styrene) insulation panels, aerated concrete bricks, or reinforced concrete beams, the coating enabled visual detection of crack formation, growth, and closure. Local color changes encoded information

about crack shape, size, and propagation path. Simple imaging provides qualitative data, with spectrophotometry providing quantitative strain measurements. The authors argue that such coatings could offer cost-effective, scalable solutions for building maintenance and repair [166]. Although this lab-scale research involved coating only the structural elements of buildings (i.e., partial packaging), it is conceptually plausible to imagine a whole construction (i.e., very large solid payloads) being packaged with this responsive packaging material to provide continuous, distributed strain sensing at the building scale.

## 7 | Current and Future Challenges and Opportunities

Despite remarkable advancements in packaging technology, several pressing challenges remain to be addressed. Below, we identify six areas where existing packaging strategies may be strengthened, or entirely new concepts may be required. We view these challenges as exciting opportunities for future research and development, and we discuss some directions that may be followed to fulfill these needs.

### 7.1 | Interfaces and Payload–Packaging Material Interactions

At the payload length scales considered here (roughly  $\sim 100\ \mu\text{m}$ –1 cm), interfacial phenomena (e.g., adsorption, wetting, capillarity, charge accumulation) are central to packaging formation and performance, either alone or coupled with bulk transport phenomena (e.g., diffusion, flow). Interfacial phenomena determine payload–packaging material interactions, and they must be favorable for packaging to occur in the first place [103]. Moreover, they regulate the interactions between the packaging material and the surrounding phase. These interactions are critical for both cases, where the payload must be hermetically sealed to prevent interaction with the environment [41], or when controlled payload release is desired, even in an anisotropic manner [58].

Chemical and physicochemical interactions between the payload and both the packaging material and the environment are equally critical. First, all materials involved must be chemically compatible to avoid unwanted reactions. Additionally, physicochemical interactions between these materials are also critical because they may, for example, control structure formation. De Luna et al. discussed initiated chemical vapor deposition onto liquids, analyzing how interactions between deposited polymers and the liquid substrate govern the morphology of the resulting material. Monomer solubility in the liquid substrate determines where polymerization occurs and the polymer material structure. Insoluble monomers react at the liquid–gas interface, resulting in a polymer film. Soluble monomers polymerize at both the free interface and in bulk, leading to a material comprising both polymer and (substrate) liquid. The spreading behavior of the polymer at the fluid interface dictates whether continuous films or discrete particles form. Positive spreading coefficients lead to polymer films, whereas negative spreading coefficients result in polymer chains aggregating at the fluid interface, typically yielding polymer particles. Monomers that undergo crosslinking may add further control by bridging adjacent chains and giving rise to a microstructured polymer film. The structure of the

crosslinked polymer network is also affected by chain diffusion and aggregation, as shown by the influence of substrate viscosity on film roughness [167].

This discussion illustrates the key role of both physical and chemical interactions in packaging at the scales considered here. A solid understanding of these effects enables engineering of payload–package–environment couplings to meet specific functional requirements. As discussed in the following, these interactions span multiple characteristic length scales, linking nanoscale processes to mesoscopic and macroscopic performance.

### 7.2 | Multiscale Integration

At the atomic/molecular scale, chemistry dictates solubility and chemical compatibility. At the molecular-to-mesoscopic scale, physicochemical interactions like adsorption or polymer–solvent affinity govern stability and morphology. Multi-scale processes are also critical. Wetting and capillarity depend on molecular-level surface energies but manifest at the mesoscale, e.g., in the shape of drops. Bulk processes like flow and diffusion depend on nanoscale permeation pathways, yet define macroscopic packaging performance. Packaging at  $\sim 100\ \mu\text{m}$ –1 cm thus inevitably involves the coupling of processes across this hierarchy of scales. The challenge, and opportunity, is to exploit this coupling deliberately, so that structural features and functionalities at one scale reinforce or complement those at others.

Several examples already discussed here illustrate how packaging strategies inherently integrate across scales. Liquid marbles [31] provide a representative case: their stability relies on the surface chemistry of individual particles at the nanometric scale, which defines their wettability and thus affinity for the fluid interface. Particles with suitable wettability spontaneously adsorb and self-organize into a *quasi*-2D layer at mesoscopic scales, which serves as the packaging material enclosing a macroscopic liquid payload. In contrast, in-situ polymer synthesis (e.g., chemical vapor deposition [102] or interfacial polymerization [24]) exemplifies a chemical route to multiscale integration. Here, molecular-scale reactivity and transport of monomers dictate where and how chains form, while mesoscopic phase separation determines whether the growing material consolidates, e.g., into films or dispersed particles [102]. The final packaging materials, often continuous macroscopic membranes, directly reflect this interplay of nanoscale chemistry and mesoscale dynamics. These bottom-up approaches are complemented by top-down strategies, such as micro- [58] and macro- [68] fabrication. In these cases, physicochemical phenomena involving properties at the nano- and micrometer levels (e.g., magnetism [58] or interfacial energy [68]) are deliberately harnessed to impose structure and function at the device or centimeter scale [66, 168]. Together, these examples emphasize that no single scale is sufficient to explain or control packaging phenomena: effective engineering requires integrating atomic, molecular, mesoscopic, and macroscopic processes within a coherent framework.

Despite these opportunities, challenges in multiscale integration into robust packaging strategies persist. A first difficulty arises from the lack of direct transferability between scales: nanoscale interactions often display emergent behaviors at mesoscopic or macroscopic levels that are challenging to predict quantitatively. For instance, the same surface modification modulating wetting

at the particle scale may lead to undesirable aggregation or phase separation at larger scales [169]. A second challenge stems from the competition between the characteristic timescales of different processes. Polymerization, diffusion, and interfacial self-assembly rarely occur in synchrony [24], and controlling one process without perturbing another remains nontrivial. Additionally, integrating bottom-up with top-down strategies requires reconciling fundamentally different design philosophies: One exploits spontaneous processes, and the other imposes external order. Finally, the inherent heterogeneity of many packaging systems, often involving soft matter, multiphase environments, and dynamic interfaces (Table 1), further complicates scaling laws and predictive modeling. Yet, these very difficulties highlight avenues for innovation. Advanced experimental techniques are increasingly capable of resolving dynamics across multiple scales, revealing how molecular events cascade into macroscopic behavior [170]. Similarly, multiscale simulation frameworks bridge atomistic descriptions with continuum models, providing unprecedented predictive power [171]. From a materials engineering perspective, programmable and stimuli-responsive systems open the door to packaging materials that actively adapt their interactions across scales rather than passively inherit them [172, 173]. Thus, while multiscale integration remains a challenge, it also represents fertile ground for breakthroughs that could redefine how payload packaging is conceived and implemented, as discussed below.

### 7.3 | The Concept of Smart Packaging

Packaging in the food and pharmaceutical industry ensures product quality and safety. This and other types of current industrial packaging are thus largely neutral, enabling basic containment with minimal functionality, e.g., transparency to allow visual inspection. At the length scales considered here, such single functionalities are often integrated into the packaging material, enabling applications like lab-in-a-drop platforms [51]. However, more advanced goals require packaging capable of communicating payload state in real time, e.g., through responsive indicators of freshness, contamination, or structural integrity [29, 146, 147, 154]. This is especially relevant for high-value payloads, such as high-cost active ingredients in drugs. Although multifunctional or responsive strategies exist (Table 1), they are typically limited to a single, pre-engineered task (e.g., one-time-use pH-responsive gas marbles [39]) and cannot be modified after fabrication. In Section 1, we introduced smart packaging, a concept that would exploit the highest level of complexity to deliver the highest level of usability.

Smart packaging aims to overcome these limitations by integrating multiple functionalities and adaptive responsiveness in a single system. It may emerge by combining multiple functionalities and responsiveness (to either payload- or environment-related stimuli), in a single platform. Some elements of this concept have been separately demonstrated. Responsiveness has been integrated using stimuli-responsive packaging materials; examples are magnetically actuated liquid marbles [85], pH-sensitive gas marbles [39], or voltage-controlled liquid lenses [50]. The monitoring of structural health with responsive coatings of liquid crystal elastomers can be extended to a truly smart packaging cargo platform [166]. A water-soluble nanocomposite ink label allowing for real-time cargo tracking via an easily readable colored QR

code that also contained concealed anti-counterfeiting elements was recently developed by nanoimprint lithography. The structural color of the material was due to self-organized hydroxypropyl cellulose; TiO<sub>2</sub> nanoparticles were added to increase the refractive index. The color change, visible to the naked eye, in 300 nm-thick QR codes indicated the humidity levels experienced by packaged fruits. This sensing enables the realization of sustainable cargo labeling, directing up-to-date product information even on commercial plastics [174]. Photonic liquid marbles also undergo color changes in response to thermal, mechanical, or chemical stimuli; however, the visible color change originates from the responsive complex-fluid payload, whereas the packaging material remains passive [35].

Despite the progress to date, combining multiple responses in a single packaging system remains largely unexplored. Implementing materials -either in the payload or packaging material, or both- that combine optical, thermal, mechanical, or barrier functions with responsiveness (pH, light, fields, mechanical stress) is a key step toward smart packaging. Soft materials, characterized by pronounced response to small perturbations, offer unique opportunities in this context. The numerous examples of soft matter engineering to make materials with multiple functionalities and responsiveness highlight many interesting possibilities. First, soft materials can reconfigure or change shape [69, 70]. This dynamic property could be exploited for designing packaging materials that can change in time (responding to growth, pressure, or environmental cues), to accommodate payload needs (e.g., expandable capsules, tunable permeability, self-healing barriers). Second, some soft materials, like polymers, can self-heal [175]. This could be exploited to engineer packaging materials that maintain integrity even after transient damage, ensuring payload safety. Third, some soft materials can self-report [71]. This could add another dimension to smart packaging by developing advanced packaging materials able to regulate the internal payload environment autonomously, without user intervention. These properties suggest that soft-matter-based smart packaging can go beyond single-use, single-function systems toward adaptive, multifunctional platforms capable of dynamic interaction with their payload and environment.

### 7.4 | Packaging for Extreme Environments

An additional challenge in packaging development is to engineer materials that remain reliable under conditions far harsher than those encountered in everyday applications. An example of an extreme terrestrial environment where packaging is essential for critical technology to function is solar energy generation in deserts. Despite energy abundance, dust accumulation severely degrades photovoltaic panel performance. Particulate accumulation on sensitive interfaces (e.g., optical elements, electrodes) of various devices is a common problem leading to gradual performance loss. Conventional dust mitigation relies on mechanical cleaning or sacrificial coatings, both of which are unsustainable under continuous exposure. Advanced soft materials offer a more resilient route, as exemplified by coatings based on polymerized liquid crystals, where surface topography changes upon electric field application. The resulting vibrations transport dust and debris across the coating and eventually remove them, providing self-cleaning functionality under both dry and humid conditions [176].

A striking example of an extreme extraterrestrial environment where dust effects are also pronounced is the Moon. Lunar regolith, the electrostatically charged granular material covering the lunar surface, adheres strongly to numerous surfaces, threatening astronaut health and impairing sensitive instruments like optical detectors [177]. NASA's Artemis and CNSA's China Manned Space Program aim to return humans there, an ambition calling for infrastructure and habitat development. Hence, packaging materials that suppress regolith accumulation onto humans or instruments (e.g., protective coatings on astronaut suits and devices, respectively), ensuring mission safety and success, will play a central role. Concepts from interface science are also useful here: the Lotus leaf, with its dual-scale roughness and low-surface-energy, exemplifies how natural designs achieve extreme repellency, inspiring synthetic analogs for dust-mitigating coatings and membranes suitable for space applications [178].

The above discussion highlights the need for packaging systems that combine functionality with robustness to survive extreme conditions. Any materials used in space applications must be resistant to extreme temperatures (and temperature variations), ultrahigh vacuum, radiation of various types (e.g., UV photons, hard X-rays, particles), and micrometeoroid impact [179]. While such requirements are well recognized at large scales (e.g., devices and infrastructure), the same needs apply at the much smaller scales considered here. For instance, samples collected in space and returned to Earth must be enclosed within packaging that can withstand extreme mechanical and environmental stresses; currently, such missions rely on highly complex and costly protocols [180].

Soft matter may provide the basis for resilient materials capable of addressing the above challenges, both in space and terrestrial settings. Self-healing polymer systems may be used to mitigate damage from micro-meteoroids, e.g., encountered in sample-return missions. A liquid healing agent may be employed as an additive, resulting in a material capable of only single healing events; however, the liquid must be compatible with the harsh conditions encountered [55]. Alternatively, healing functionality can be embedded directly in a polymer network via reversible chemical or physical bonds, leading to a system capable of recovering from transient failures several times [181]. Concerning UV radiation, polymers and composites employing organic UV absorbers and inorganic nanoparticle fillers can absorb harmful radiation while preserving mechanical and optical integrity. These materials offer a route to resilient packaging for safeguarding sensitive payloads under prolonged irradiation and harsh thermal cycling [182]. Finally, polymer-based systems such as epoxy-cyanate ester blends, bioderived high-glass transition epoxies, and phthalonitrile resins show that tailored network rigidity and elevated glass transition temperatures can maintain structural integrity well above 200°C [183]. These advances illustrate how materials, originally developed for other applications, in this case high-temperature electronic and power-module encapsulation, can be translated into robust packaging strategies capable of tolerating extreme environmental conditions.

These examples demonstrate how soft materials can be engineered to form the basis of robust packaging strategies suitable for extreme environments. At the same time, these strategies emphasize the importance of designing solutions that are not only technically effective but also practical and scalable, paving

the way for accessible packaging approaches that combine performance with ease of implementation. In spite of their potential, soft materials also have limitations, particularly when space technologies are considered. Polymers in particular, due to molecular mobility, low thermal stability, and susceptibility to bond scission, are far more vulnerable than hard materials like metals or ceramics. Severe thermal swings induce embrittlement, creep, and cracking; ultrahigh vacuum drives outgassing and loss of plasticizers; high-energy radiation causes chain scission, cross-linking, and optical or mechanical degradation. Furthermore, micrometeoroid impacts can readily penetrate or erode polymer-based components due to their low density and low modulus, posing a major challenge for long-term reliability. Despite these vulnerabilities, polymers remain valuable in extreme-environment technologies when they are properly shielded, chemically stabilized, or structurally engineered to withstand the specific stressors in a given application.

## 7.5 | Accessible Packaging Solutions

The development of advanced packaging solutions often relies on complex and costly equipment or strictly controlled conditions. For instance, top-down strategies like metal nanocontainers [58] require photolithography in clean-room environments. Bottom-up approaches like physical vapor deposition of metal films [55] or chemical vapor deposition of polymers [50] typically necessitate vacuum systems; even when pressure requirements are relaxed, elaborate instrumentation remains necessary [49]. Other strategies depend on materials not easily accessible; for example, many chemically modified nanoparticles used to stabilize liquid marbles are not commercially available or cannot be produced at scale (Table 1), and some otherwise accessible materials rely on potentially harmful solvents [51]. While certain packaging challenges may inevitably employ such specialized methods, more accessible solutions are often desirable, especially when aiming for widespread adoption.

Soft matter and interface science concepts, combined with readily accessible assembly strategies, can help address these limitations. Both bottom-up approaches (e.g., self-assembly, phase separation) and top-down techniques (e.g., additive manufacturing) provide practical routes to functional packaging. Electrolyte-induced gelation of natural polysaccharides [53] or destabilization of particle rafts at liquid surfaces [32] exploit fundamental interfacial phenomena to package liquid payloads without sophisticated instruments. Magnetic capillary containers [68] illustrate how an accessible manufacturing tool like 3D printing, combined with wettability engineering, can yield smart, responsive packages capable of containing diverse liquids under different environmental conditions. Even simpler approaches are also possible, as shown by WRAPPINGS that requires only standard equipment to produce, on demand, packages for liquid or gas payloads functioning as lab-in-a-drop or lab-in-a-bubble systems. Remarkably, besides water, only low-cost, nontoxic materials—found even in everyday products—are used to form biodegradable and biocompatible polymer films [24], demonstrating that accessible systems can simultaneously meet performance, safety, and sustainability criteria. Taken together with other examples discussed earlier (e.g., biopolymers [53], bio-based nanoparticles [66], natural granular materials [32]), they highlight a broader advantage of soft matter: it encompasses a plethora of abundant

materials suitable for sustainable packaging, while enabling the integration of advanced functions like responsiveness and sensing.

## 7.6 | Sustainability, End-of-Life, Scalability, and Cost

We have so far analyzed how fundamental physical and chemical phenomena may be engineered across length scales to design packaging solutions with advanced features. The use of accessible fabrication methods and materials further adds a practical dimension to their development. However, to systematically advance packaging solutions, performance must be complemented by additional attributes increasingly dictated by environmental and energy concerns, most notably sustainability and end-of-life considerations (including recycling and degradability). At the same time, to attract industrial interest, packaging strategies must also be cost-effective and readily scalable.

Environmental concerns demand a shift towards recyclable, biodegradable, or bio-based packaging materials. Promising candidates include cellulose-based films, starch-based matrices, biopolymer composites, and clay-based hybrids, many of which show barrier, mechanical, or optical properties relevant to packaging [35, 36, 123, 152, 133, 140, 150, 153, 184]. For instance, the use of fibrous waste cotton and pollen shells to create a fiber/particle slurry in water, ethanol, and sodium hydroxide yields a robust bioplastic that can be reshaped simply by re-soaking in water. This eliminates toxic reagents and energy-intensive reprocessing steps and leads to a favorable life cycle profile across preparation, processing, and recycling [185]. Another promising material type is transparent, low-temperature moldable plastics based on poly(ethyl cyanoacrylate). These systems enable closed-loop recycling with recovery rates above 90%, even when mixed with common commercial plastics (e.g., poly(ethylene), poly(propylene), poly(styrene)) [186]. Complementary to these polymer-based routes, hybrid systems like polymer–clay nanocomposites also show great potential. Multilayer polymer–clay ultrathin films prepared *via* solution-based assembly exhibit remarkable gas-barrier properties while maintaining transparency, being highly attractive for sustainable packaging applications where both environmental compatibility and functional performance are required [25].

To enable industrial adoption of multifunctional and smart packaging, production methods must be not only innovative but also scalable and cost-effective. Roll-to-roll coating for the continuous deposition of cellulose nanofibers onto paperboard shows how renewable materials can be processed at a commercial scale while maintaining competitive costs and barrier performance [187]. Additive manufacturing is also emerging as a versatile route that shows promise for sustainable soft-material packaging at scale. Ongoing research focuses on processing natural and bio-derived polymers into various forms suitable for additive manufacturing, such as filaments for extrusion-based 3D printing, photosensitive resins and inks for vat photopolymerization, jet printing, and direct ink writing processes, as well as powders for selective laser sintering [188]. Digital printing technologies further expand this toolbox: Inkjet printing is highly promising for developing packaging materials with smart features as it can rapidly deposit functional inks. Although more research is

required to achieve commercialization levels for this approach, its high efficiency, low cost, and scalability show strong potential [189]. Scaling, however, cannot come at the expense of sustainability. Solutions that are “green but expensive” will remain commercially unattractive, while unsustainable cost-cutting undermines circularity. The most impactful strategies will thus balance raw material cost, processing efficiency, and end-of-life considerations, while aligning with existing infrastructure. This balance will enable today’s lab demonstrations to evolve into packaging platforms that are not only functional and sustainable, but also economically competitive.

## 8 | Summary and Take-Home Messages

This review surveyed packaging strategies developed for macroscopic payloads in the  $\sim 100\ \mu\text{m}$  to  $\sim 1\ \text{cm}$  size range ( $\sim\text{pL}$  to  $\sim\text{mL}$  volumes), organizing the field through a framework based on payload phase (liquid, gas, solid) and packaging function. We distinguished neutral packaging that merely contains the payload, functional packaging that imparts properties like optical transparency or controlled payload release, and responsive packaging that adapts to stimuli, enabling additional functions like programmable release or real-time sensing. Within this structure, we argued that future progress depends on integrating multiple functionalities with responsiveness to create truly smart packaging strategies. Our analysis identified recurring scientific and engineering challenges, e.g., predicting and manipulating interfacial, mechanical, and transport phenomena across scales; translating them into manufacturable architectures; ensuring sustainability, recyclability, scalability, and cost-effectiveness. Soft matter emerges as a particularly promising platform [190, 191], offering versatile building blocks (e.g., polymers, liquid crystals, colloids, gels, granular media) and conceptual mechanisms needed to engineer macroscopic, adaptive packaging platforms.

Two take-home messages emerge clearly. First, smart packaging at these scales is intrinsically interdisciplinary: Addressing the coupled material, interfacial, mechanical, chemical, and processing requirements will require contributions from soft-matter physics, materials science, interfacial engineering, food and pharmaceutical technology, and manufacturing science, alongside sustainability and regulatory expertise. Second, progress depends strongly on open-mindedness and cross-fertilization of ideas. Strategies can arise from diverse inspirations, whether from nature (e.g., the Lotus leaf effect), interfacial and colloid science, advanced microfabrication, programmable soft matter, or even playful systems like soap bubbles. True collaboration and receptiveness to ideas, regardless of origin, will be essential to advance truly smart, practical, and sustainable packaging technologies capable of meeting the environmental and functional demands of future societies.

Looking ahead, the packaging field will increasingly converge on platforms combining five key attributes identified here: (i) precise interfacial control to stabilize various payloads; (ii) adaptive mechanical response to tolerate deformation, shock, and environmental fluctuations; (iii) regulated mass and energy transport for protection, release, or sensing; (iv) packaging material sustainability through biodegradability, recyclability, or circular feedstocks; and (v) compatibility with scalable manufacturing,

from roll-to-roll processing to additive manufacturing techniques. Achieving these properties simultaneously will require (soft) materials with programmable structure and function, supported by multiscale modeling, automated formulation tools, and closed-loop experimental design. As these systems move from isolated demonstrations to integrated material–architecture concepts, responsiveness, sustainability, and manufacturability will need to be designed together rather than added sequentially. Soft matter platforms are well positioned to drive this evolution, but must be mechanically, thermally, and chemically reinforced to survive the harsh conditions in emerging applications, e.g., those in extreme environments. This will likely demand hybrid systems that combine soft matter with high-performance materials like inorganic barriers, fiber-reinforced architectures, or architected metamaterials capable of providing toughness without sacrificing functionality. Such synergies shall provide the foundations for the next-generation packaging technologies across biomedical, energy, environmental, and space applications.

### Author Contributions

**Venkata S. R. Jampani:** conceptualization (equal), data curation (equal), funding acquisition (equal), project administration (equal), visualization (equal), writing – original draft (equal), writing – review and editing (equal). **Manos Anyfantakis:** conceptualization (equal), data curation (equal), funding acquisition (equal), investigation (equal), project administration (equal), resources (equal), visualization (equal), writing – original draft (equal), writing – review and editing (equal).

### Funding

This study was supported by the javna agencija za znanstvenoraziskovalno in inovacijsko dejavnost republike Slovenije (ARIS) project numbers: N1-0400, P1-0099, COST (European Cooperation in Science and Technology) CA24126 (VSRJ) and Fonds National de la Recherche Luxembourg (C18/MS/12701231) (MA). The authors acknowledge the kind support from Jan Lagerwall and the Experimental Soft Matter Physics Group at the University of Luxembourg, where some of the research discussed here was pursued. The authors thank Joze Luzar for providing helium.

### Conflicts of Interest

The authors declare no conflicts of interest.

### Data Availability Statement

Data sharing is not applicable to this article as no datasets were generated or analyzed during the current study.

### References

1. G. L. Robertson, *Food Packaging* (CRC Press, 2005).
2. E. G. Schutt, D. H. Klein, R. M. Mattrey, and J. G. Riess, “Injectable Microbubbles as Contrast Agents for Diagnostic Ultrasound Imaging: The Key Role of Perfluorochemicals,” *Angewandte Chemie International Edition* 42 (2003): 3218.
3. P. Walstra, P. Walstra, J. T. M. Wouters, and T. J. Geurts, *Dairy Science and Technology* (CRC Press, 2005).
4. R. C. Chandan, *Manufacturing Yogurt and Fermented Milks* (Wiley, 2013).
5. A. D. Karaman, B. Özer, M. A. Pascall, and V. Alvarez, “Recent Advances in Dairy Packaging,” *Food Reviews International* 31 (2015): 295.

6. M. G. Kontominas, “Packaging and the Shelf Life of Milk: Recent Developments,” in *Reference Module in Food Science* (Elsevier, 2019).
7. D. X. Li, Y. K. Oh, S. J. Lim, et al., “Novel Gelatin Microcapsule with Bioavailability Enhancement of Ibuprofen Using Spray-Drying Technique,” *International Journal of Pharmaceutics* 355 (2008): 277.
8. A. D. Dinsmore, M. F. Hsu, M. G. Nikolaidis, M. Marquez, A. R. Bausch, and D. A. Weitz, “Colloidosomes: Selectively Permeable Capsules Composed of Colloidal Particles,” *Science* 298 (2002): 1006.
9. S. F. M. Van Dongen, H. P. M. De Hoog, R. J. R. W. Peters, M. Nallani, R. J. M. Nolte, and J. C. M. Van Hest, “Biohybrid Polymer Capsules,” *Chemical Reviews* 109 (2009): 6212.
10. S. Frazier, X. Jiang, and J. C. Burton, “How to Make a Giant Bubble,” *Physical Review Fluids* 5 (2020): 013304.
11. E. Kang, H. S. Min, J. Lee, et al., “Nanobubbles from Gas-Generating Polymeric Nanoparticles: Ultrasound Imaging of Living Subjects,” *Angewandte Chemie—International Edition* 49 (2010): 524.
12. D. Řepka, A. Kurillová, Y. Murtaja, and L. Lapčik, “Application of Physical-Chemical Approaches for Encapsulation of Active Substances in Pharmaceutical and Food Industries,” *Foods* 12 (2023): 2189.
13. Y. Lv, N. Liu, C. Chen, Z. Cai, and J. Li, “Pharmaceutical Packaging Materials and Medication Safety: A Mini-Review,” *Safety* 11 (2025): 69.
14. K. Marsh and B. Bugusu, “Food Packaging—Roles, Materials, and Environmental Issues,” *Journal of Food Science* 72 (2007): R39.
15. J. Yammine, N.-E. Chihib, A. Gharsallaoui, A. Ismail, and L. Karam, “Advances in Essential Oils Encapsulation: Development, Characterization and Release Mechanisms,” *Polymer Bulletin* 81 (2024): 3837.
16. J. P. F. Carvalho, C. S. R. Freire, and C. Vilela, *Sustainable Food Processing and Engineering Challenges* (Elsevier, 2021): 315.
17. C. Vasile, “Polymeric Nanocomposites and Nanocoatings for Food Packaging: A Review,” *Materials* 11 (2018): 1834.
18. B. Kuswandi, “Environmental Friendly Food Nano-Packaging,” *Environmental Chemistry Letters* 15 (2017): 205.
19. M. del R. Herrera-Rivera, S. P. Torres-Arellanes, C. I. Cortés-Martínez, et al., “Nanotechnology in Food Packaging Materials: Role and Application of Nanoparticles,” *RSC Advances* 14 (2024): 21832.
20. A. Ahuja, P. Samyn, and V. K. Rastogi, “Paper Bottles: Potential to Replace Conventional Packaging for Liquid Products,” *Biomass Conversion and Biorefinery* 14 (2024): 13779.
21. M. A. Hubbe, A. Ferrer, P. Tyagi, et al., “Nanocellulose in Thin Films, Coatings, and Plies for Packaging Applications: A Review,” *Bioresources* 12 (2016): 2143.
22. M. Leman, F. Abouakil, A. D. Griffiths, and P. Tabeling, “Droplet-Based Microfluidics at the Femtolitre Scale,” *Lab on a Chip* 15 (2015): 753.
23. D. Li, Q. Luo, Q. Liu, et al., “Edible Cellulose-Based Photonic Crystals with Low-Temperature Response for Food Sensing,” *Carbohydrate Polymers* 367 (2025): 124029.
24. V. S. R. Jampani, M. Škarabot, U. Mur, et al., “Water-Templated Growth of Interfacial Superglue Polymers for Tunable Thin Films and In Situ Fluid Encapsulation,” *Advanced Materials* 36 (2024): 2408243.
25. M. A. Priolo, D. Gamboa, K. M. Holder, and J. C. Grunlan, “Super Gas Barrier of Transparent Polymer–Clay Multilayer Ultrathin Films,” *Nano Letters* 10 (2010): 4970.
26. A. Sorrentino, *Nanocoatings and Ultra-Thin Films* (Elsevier, 2011): 203.
27. A. Kang, J. Park, J. Ju, G. S. Jeong, and S.-H. Lee, “Cell Encapsulation via Microtechnologies,” *Biomaterials* 35 (2014): 2651.
28. P. Kumar, S. Tripathi, D. Ramakanth, and K. K. Gaikwad, “Novel Ethylene Scavenger Based on Sillimanite and Bentonite Clay for

- Packaging Applications: A Sustainable Alternative for Preservation of Fresh Produce,” *Sustainable Chemistry and Pharmacy* 38 (2024): 101516.
29. L.-T. Wu, I.-L. Tsai, Y.-C. Ho, et al., “Active and Intelligent Gellan Gum-Based Packaging Films for Controlling Anthocyanins Release and Monitoring Food Freshness,” *Carbohydrate Polymers* 254 (2021): 117410.
30. B. P. Binks and S. O. Lumsdon, “Influence of Particle Wettability on the Type and Stability of Surfactant-Free Emulsions,” *Langmuir* 16 (2000): 8622.
31. P. Aussillous and D. Quéré, “Liquid Marbles,” *Nature* 411 (2001): 924.
32. M. Abkarian, S. Protière, J. M. Aristoff, and H. A. Stone, “Gravity-Induced Encapsulation of Liquids by Destabilization of Granular Rafts,” *Nature Communications* 4 (2013): 1895.
33. M. A. Augustin and Y. Hemar, “Nano- and Micro-Structured Assemblies for Encapsulation of Food Ingredients,” *Chemical Society Reviews* 38 (2009): 902.
34. J. S. Lee and J. Feijen, “Polymersomes for Drug Delivery: Design, Formation and Characterization,” *Journal of Controlled Release* 161 (2012): 473.
35. M. Anyfantakis, V. S. R. Jampani, R. Kizhakidathazhath, B. P. Binks, and J. P. F. Lagerwall, “Responsive Photonic Liquid Marbles,” *Angewandte Chemie* 132 (2020): 19422.
36. P. J. A. Sobral, F. C. Menegalli, M. D. Hubinger, and M. A. Roques, “Mechanical, Water Vapor Barrier and Thermal Properties of Gelatin Based Edible Films,” *Food Hydrocolloids* 15 (2001): 423.
37. K. P. Seremeta and A. Sosnik, *Nanotechnology for Oral Drug Delivery* (Elsevier, 2020), 199.
38. B. P. Binks and R. Murakami, “Phase Inversion of Particle-Stabilized Materials From Foams to Dry Water,” *Nature Materials* 5 (2006): 865.
39. T. Yasui, A. Fameau, H. Park, et al., “Stimulus-Responsive Gas Marbles as an Amphibious Carrier for Gaseous Materials,” *Advanced Science* 11 (2024): 2404728.
40. M. Kotsidi, G. Gorgolis, M. G. P. Carbone, et al., “Preventing Colour Fading in Artworks with Graphene Veils,” *Nature Nanotechnology* 16 (2021): 1004.
41. A. Yulaev, A. Lipatov, A. X. Lu, A. Sinitskii, M. S. Leite, and A. Kolmakov, “Imaging and Analysis of Encapsulated Objects through Self-Assembled Electron and Optically Transparent Graphene Oxide Membranes,” *Advanced Materials Interfaces* 4 (2017): 1600734.
42. D. Kumar, J. D. Paulsen, T. P. Russell, and N. Menon, “Wrapping with a Splash: High-Speed Encapsulation with Ultrathin Sheets,” *Science* 359 (2018): 775.
43. J. Yang, Z. Z. Zhang, X. H. Men, and X. H. Xu, “Superoleophobicity of a Material Made From Fluorinated Titania Nanoparticles,” *Journal of Dispersion Science and Technology* 32 (2011): 485.
44. V. Sivan, S. Y. Tang, A. P. O’Mullane, et al., “Liquid Metal Marbles,” *Advanced Functional Materials* 23 (2013): 144.
45. J. Tian, N. Fu, X. D. Chen, and W. Shen, “Respirable Liquid Marble for the Cultivation of Microorganisms,” *Colloids and Surfaces. B, Biointerfaces* 106 (2013): 187.
46. X. Li, Y. Xue, P. Lv, et al., “Liquid Plasticine: Controlled Deformation and Recovery of Droplets with Interfacial Nanoparticle Jamming,” *Soft Matter* 12 (2016): 1655.
47. F. Geyer, Y. Asaumi, D. Vollmer, H. Butt, Y. Nakamura, and S. Fujii, “Polyhedral Liquid Marbles,” *Advanced Functional Materials* 29 (2019): 1808826.
48. Y. Kawamura, H. Mayama, and Y. Nonomura, “Edible Liquid Marbles and Capsules Covered with Lipid Crystals,” *Journal of Oleo Science* 61 (2012): 477.
49. F. Rezaei, M. D. Dickey, and P. J. Hauser, “Polymeric Encapsulation of Liquids via Plasma Surface Polymerization,” *Journal of Applied Polymer Science* 137 (2020): 48880.
50. N. Binh-Khiem, K. Matsumoto, and I. Shimoyama, “Polymer Thin Film Deposited on Liquid for Varifocal Encapsulated Liquid Lenses,” *Applied Physics Letters* 93 (2008): 124101.
51. S. Coppola, G. Nasti, V. Vespini, et al., “Quick Liquid Packaging: Encasing Water Silhouettes by Three-Dimensional Polymer Membranes,” *Science Advances* 5 (2019): eaat5189.
52. N. Bremond, E. Santanach-Carreras, L. Y. Chu, and J. Bibette, “Formation of Liquid-Core Capsules Having a Thin Hydrogel Membrane: Liquid pearls,” *Soft Matter* 6 (2010): 2484.
53. W. Song, A. C. Lima, and J. F. Mano, “Bioinspired Methodology to Fabricate Hydrogel Spheres for Multi-Applications Using Superhydrophobic Substrates,” *Soft Matter* 6 (2010): 5868.
54. C. Py, P. Reverdy, L. Doppler, J. Bico, B. Roman, and C. N. Baroud, “Capillary Origami: Spontaneous Wrapping of a Droplet with an Elastic Sheet,” *Physical Review Letters* 98 (2007): 2.
55. E. F. Borra, O. Seddiki, R. Angel, et al., “Deposition of Metal Films on an Ionic Liquid as a Basis for a Lunar Telescope,” *Nature* 447 (2007): 979.
56. T. Takei, Y. Yamasaki, Y. Yuji, et al., “Millimeter-Sized Capsules Prepared Using Liquid Marbles: Encapsulation of Ingredients with High Efficiency and Preparation of Spherical Core-Shell Capsules with Highly Uniform Shell Thickness Using Centrifugal Force,” *Journal of Colloid and Interface Science* 536 (2019): 414.
57. M. Cui, T. Emrick, and T. P. Russell, “Stabilizing Liquid Drops in Nonequilibrium Shapes by the Interfacial Jamming of Nanoparticles,” *Science* 342 (2013): 460.
58. T. Leong, Z. Gu, T. Koh, and D. H. Gracias, “Spatially Controlled Chemistry Using Remotely Guided Nanoliter Scale Containers,” *Journal of the American Chemical Society* 128 (2006): 11336.
59. S. Misra, K. Trinavee, N. S. K. Gunda, and S. K. Mitra, “Encapsulation with an Interfacial Liquid Layer: Robust and Efficient Liquid-Liquid Wrapping,” *Journal of Colloid and Interface Science* 558 (2020): 334.
60. Y. Timounay, O. Pitois, and F. Rouyer, “Gas Marbles: Much Stronger than Liquid Marbles,” *Physical Review Letters* 118 (2017): 228001.
61. E. Mukai, C. Dari, T. Yasui, T. Yagishita, A. Fameau, and S. Fujii, “Cinnamon Particle-Stabilized Gas Marbles: A Novel Approach for Enhanced Stability and Versatile Applications,” *Advanced Functional Materials* 35 (2025): 2409926.
62. M. Eguchi, M. Konarova, N. L. Torad, et al., “Highly Adhesive and Disposable Inorganic Barrier Films: Made From 2D Silicate Nanosheets and Water,” *Journal of Materials Chemistry A* 10 (2022): 1956.
63. A. Brackmann, J. Streif, and F. Bangerth, “Relationship between a Reduced Aroma Production and Lipid Metabolism of Apples after Long-Term Controlled-Atmosphere Storage,” *Journal of the American Society for Horticultural Science* 118 (1993): 243.
64. E. C. dos Santos, Z. Rozynek, E. L. Hansen, et al., “Ciprofloxacin Intercalated in Fluorohectorite Clay: Identical Pure Drug Activity and Toxicity with Higher Adsorption and Controlled Release Rate,” *RSC Advances* 7 (2017): 26537.
65. R. Giorgi, L. Dei, M. Ceccato, C. Schettino, and P. Baglioni, “Nanotechnologies for Conservation of Cultural Heritage: Paper and Canvas Deacidification,” *Langmuir* 18 (2002): 8198.
66. R. Abouzeid, P. Sadeghi, D. H. Picha, and Q. Wu, “Sustainable Nanocoatings for Agricultural Produce: A Biodegradable Approach Using Cellulose Nanomaterials and Pectin From Sweet Potato Peel,” *Carbohydrate Polymer Technologies and Applications* 10 (2025): 100785.
67. K. Aono, K. Ueno, S. Hamasaki, et al., ““Foam Marble” Stabilized with One Type of Polymer Particle,” *Langmuir* 38 (2022): 7603.

68. Y. Zhang, Z. Huang, Z. Cai, et al., "Magnetic-Actuated "capillary Container" for Versatile Three-Dimensional Fluid Interface Manipulation," *Science Advances* 7 (2021): 7498.
69. K. Peddireddy, S. Čopar, K. V. Le, I. Mušević, C. Bahr, and V. S. R. Jampani, "Self-Shaping Liquid Crystal Droplets by Balancing Bulk Elasticity and Interfacial Tension," *Proceedings of the National Academy of Sciences* 118 (2021): e2011174118.
70. V. S. R. Jampani, R. H. Volpe, K. R. de Sousa, J. F. Machado, C. M. Yakacki, and J. P. F. Lagerwall, "Liquid Crystal Elastomer Shell Actuators with Negative Order Parameter," *Science Advances* 5 (2019): eaaw2476.
71. Y. K. Kim, X. Wang, P. Mondkar, E. Bukusoglu, and N. L. Abbott, "Self-Reporting and Self-Regulating Liquid Crystals," *Nature* 557 (2018): 539.
72. I.-H. H. Lin, D. S. Miller, P. J. Bertics, C. J. Murphy, J. J. de Pablo, and N. L. Abbott, "Endotoxin-Induced Structural Transformations in Liquid Crystalline Droplets," *Science* 332 (2011): 1297.
73. K. Stratford, R. Adhikari, I. Pagonabarraga, J.-C. Desplat, and M. E. Cates, "Colloidal Jamming at Interfaces: A Route to Fluid-Bicontinuous Gels," *Science* 309 (2005): 2198.
74. L. Gao and T. J. McCarthy, "Ionic Liquid Marbles," *Langmuir* 23 (2007): 10445.
75. P. Aussillous and D. Quéré, "Properties of Liquid Marbles," *Proceedings of the Royal Society A: Mathematical, Physical and Engineering Sciences* 462 (2006): 973.
76. Z. Liu, Y. Zhang, C. Chen, et al., "Larger Stabilizing Particles Make Stronger Liquid Marble," *Small* 15 (2019): 1804549.
77. P. S. Bhosale, M. V. Panchagnula, and H. A. Stretz, "Mechanically Robust Nanoparticle Stabilized Transparent Liquid Marbles," *Applied Physics Letters* 93 (2008): 034109.
78. B. P. Binks, "Particles as Surfactants—Similarities and Differences" *Current Opinion in Colloid and Interface Science* 7 (2002): 21.
79. G. McHale and M. I. Newton, "Liquid Marbles: Topical Context Within Soft Matter and Recent Progress," *Soft Matter* 11 (2015): 2530.
80. Y. Zhao, J. Fang, H. Wang, X. Wang, and T. Lin, "Magnetic Liquid Marbles: Manipulation of Liquid Droplets Using Highly Hydrophobic Fe<sub>3</sub>O<sub>4</sub> Nanoparticles," *Advanced Materials* 22 (2010): 707.
81. M. Dandan and H. Y. Erbil, "Evaporation Rate of Graphite Liquid Marbles: Comparison with Water Droplets," *Langmuir* 25 (2009): 8362.
82. E. Bormashenko, "Liquid Marbles: Properties and Applications," *Current Opinion in Colloid and Interface Science* 16 (2011): 266.
83. T. Arbatan, A. Al-Abboodi, F. Sarvi, P. P. Y. Chan, and W. Shen, "Tumor Inside a Pearl Drop," *Advanced Healthcare Materials* 1 (2012): 467.
84. L. Zhang, D. Cha, and P. Wang, "Remotely Controllable Liquid Marbles," *Advanced Materials* 24 (2012): 4756.
85. Y. Xue, H. Wang, Y. Zhao, et al., "Magnetic Liquid Marbles: A "Precise" Miniature Reactor," *Advanced Materials* 22 (2010): 4814.
86. D. Dupin, S. P. Armes, and S. Fujii, "Stimulus-Responsive Liquid Marbles," *Journal of the American Chemical Society* 131 (2009): 5386.
87. Y. Zhao, Z. Xu, H. Niu, X. Wang, and T. Lin, "Magnetic Liquid Marbles: Toward "Lab in a Droplet"," *Advanced Functional Materials* 25 (2015): 437.
88. T. T. Y. Tan, A. Ahsan, M. R. Reithofer, et al., "Photoresponsive Liquid Marbles and Dry Water," *Langmuir* 30 (2014): 3448.
89. S. Fujii, S. I. Yusa, and Y. Nakamura, "Stimuli-Responsive Liquid Marbles: Controlling Structure, Shape, Stability, and Motion," *Advanced Functional Materials* 26 (2016): 7206.
90. Q. Lv, J. Li, R. Wang, and L. Zhang, "Ultraviolet-Light-Triggered Coalescence of Liquid Marbles for Multistep Microreactions," *Particle and Particle Systems Characterization* 40 (2023): 2300076.
91. J. Vialetto, M. Hayakawa, N. Kavokine, et al., "Magnetic Actuation of Drops and Liquid Marbles Using a Deformable Paramagnetic Liquid Substrate," *Angewandte Chemie International Edition* 56 (2017): 16565.
92. M. Paven, H. Mayama, T. Sekido, H. Butt, Y. Nakamura, and S. Fujii, "Light-Driven Delivery and Release of Materials Using Liquid Marbles," *Advanced Functional Materials* 26 (2016): 3199.
93. W. Gao, H. K. Lee, J. Hobley, T. Liu, I. Y. Phang, and X. Y. Ling, "Graphene Liquid Marbles as Photothermal Miniature Reactors for Reaction Kinetics Modulation," *Angewandte Chemie* 127 (2015): 4065.
94. S. Kumar, N. Barman, A. Borbora, P. Mondal, M. Tenjimbayashi, and U. Manna, "PH-Triggered Adjustable Bursting of Liquid Marbles in Water Pools," *Journal of Materials Chemistry A* 12 (2024): 3362.
95. P. Singha, S. Swaminathan, A. S. Yadav, and S. N. Varanakkottu, "Surfactant-Mediated Collapse of Liquid Marbles and Directed Assembly of Particles at the Liquid Surface," *Langmuir* 35 (2019): 4566.
96. C. H. Ooi, R. Vadivelu, J. Jin, et al., "Liquid Marble-Based Digital Microfluidics – Fundamentals and Applications," *Lab on a Chip* 21 (2021): 1199.
97. T. Tong, H. Hu, Y. Xie, and J. Jin, "Advancements in Liquid Marbles as an Open Microfluidic Platform: Rapid Formation, Robust Manipulation, and Revolutionary Applications," *Droplet* 4 (2025): 1.
98. M. Tenjimbayashi, T. Mouterde, P. K. Roy, and K. Uto, "Liquid Marbles: Review of Recent Progress in Physical Properties, Formation Techniques, and Lab-in-a-Marble Applications in Microreactors and Biosensors," *Nanoscale* 15 (2023): 18980.
99. J. Saczek, X. Yao, V. Zivkovic, et al., "Long-Lived Liquid Marbles for Green Applications," *Advanced Functional Materials* 31 (2021): 2011198.
100. H. Gu, B. Ye, H. Ding, C. Liu, Y. Zhao, and Z. Gu, "Non-Iridescent Structural Color Pigments From Liquid Marbles," *Journal of Materials Chemistry C* 3 (2015): 6607.
101. A. B. Subramaniam, M. Abkarian, L. Mahadevan, and H. A. Stone, "Non-Spherical Bubbles," *Nature* 438 (2005): 930.
102. P. D. Haller, R. J. Frank-Finney, and M. Gupta, "Vapor-Phase Free Radical Polymerization in the Presence of an Ionic Liquid," *Macromolecules* 44 (2011): 2653.
103. S. Misra, A. Chowdhury, and S. K. Mitra, "Liquid-Liquid Encapsulation with a Constrained Interfacial Layer," *Journal of Colloid and Interface Science* 701 (2025): 138658.
104. K. Ferrara, R. Pollard, and M. Borden, "Ultrasound Microbubble Contrast Agents: Fundamentals and Application to Gene and Drug Delivery," *Annual Review of Biomedical Engineering* 9 (2007): 415.
105. H. Lee, H. Kim, H. Han, et al., "Microbubbles Used for Contrast Enhanced Ultrasound and Theragnosis: A Review of Principles to Applications," *Biomedical Engineering Letters* 7 (2017): 59.
106. E. Dickinson, "Food Emulsions and Foams Stabilization by Particles," *Current Opinion in Colloid and Interface Science* 15 (2010): 40.
107. B. S. Murray, "Recent Developments in Food Foams," *Current Opinion in Colloid and Interface Science* 50 (2020): 101394.
108. G. Debrégeas, P.-G. de Gennes, and F. Brochard-Wyart, "The Life and Death of "Bare" Viscous Bubbles," *Science* 279 (1998): 1704.
109. L. W. Schwartz and R. V. Roy, "Modeling Draining Flow in Mobile and Immobile Soap Films," *Journal of Colloid and Interface Science* 218 (1999): 309.
110. C. Cohen, B. D. Texier, E. Reyssat, J. H. Snoeijer, D. Quéré, and C. Clanet, "On the Shape of Giant Soap Bubbles," *Proceedings of the National Academy of Sciences* 114 (2017): 2515.

111. A. Roux, A. Duchesne, and M. Baudoin, "Everlasting Bubbles and Liquid Films Resisting Drainage, Evaporation, and Nuclei-Induced Bursting," *Physical Review Fluids* 7 (2022): L011601.
112. <https://soapbubble.fandom.com> (accessed: 5. 7, 2025), and the authors' own photographs depicting soap-bubble demonstrations (used in Fig. 5A(iii)). Web resource consulted: Soap Bubble Wiki (2025).
113. Y. Timounay, E. Ou, E. Lorenceau, F. Rouyer, "Low Gas Permeability of Particulate Films Slows Down the Aging of Gas Marbles," *Soft Matter* 13 (2017): 7717.
114. Y. Zhu, S. Murali, W. Cai, et al., "Graphene and Graphene Oxide: Synthesis, Properties, and Applications," *Advanced Materials* 22 (2010): 3906.
115. A. H. C. Neto, N. M. R. Peres, K. S. Novoselov, and A. K. Geim, "The Electronic Properties of Graphene," *Reviews of Modern Physics* 81 (2009): 109.
116. R. Basu and S. A. Shalov, "Graphene as Transmissive Electrodes and Aligning Layers for Liquid-Crystal-Based Electro-Optic Devices," *Physical Review E* 96 (2017): 1.
117. H. W. Kim, H. W. Yoon, S.-M. Yoon, et al., "Selective Gas Transport Through Few-Layered Graphene and Graphene Oxide Membranes," *Science* 342 (2013): 91.
118. J. S. Bunch, S. S. Verbridge, J. S. Alden, et al., "Impermeable Atomic Membranes From Graphene Sheets," *Nano Letters* 8 (2008): 2458.
119. R. K. Joshi, P. Carbone, F. C. Wang, et al., "Precise and Ultrafast Molecular Sieving Through Graphene Oxide Membranes," *Science* 343 (2014): 752.
120. J. Braeuer, J. Besser, M. Wiemer, and T. Gessner, "A Novel Technique for MEMS Packaging: Reactive Bonding with Integrated Material Systems," *Sensors and Actuators A: Physical* 188 (2012): 212.
121. P. Wu, H. Wang, Y. Tang, Y. Zhou, and T. Lu, "Three-Dimensional Interconnected Network of Graphene-Wrapped Porous Silicon Spheres: In Situ Magnesiothermic-Reduction Synthesis and Enhanced Lithium-Storage Capabilities," *ACS Applied Materials and Interfaces* 6 (2014): 3546.
122. H. Bodaghi, "Characterization and Application of the Nanocomposite Packaging Films Containing Clay and TiO<sub>2</sub> on Preservation of Tomato Fruit under Cold Storage," *BMC Plant Biology* 24 (2024): 521.
123. J. O. Fossum, "Clay Nanolayer Encapsulation, Evolving From Origins of Life to Future Technologies," *European Physical Journal Special Topics* 229 (2020): 2863.
124. A. Yurtsever, P.-X. Wang, F. Priante, et al., "Molecular Insights on the Crystalline Cellulose-Water Interfaces via Three-Dimensional Atomic Force Microscopy," *Science Advances* 8 (2022): 160.
125. D. J. Kim, Y. S. Choi, H. H. Choi, et al., "Degradation Protection of Color Dyes Encapsulated by Graphene Barrier Films," *Chemistry of Materials* 31 (2019): 7173.
126. Y. Su, V. G. Kravets, S. L. Wong, J. Waters, A. K. Geim, and R. R. Nair, "Impermeable Barrier Films and Protective Coatings Based on Reduced Graphene Oxide," *Nature Communications* 5 (2014): 4843.
127. C. Tournassat, I. C. Bourg, C. I. Steefel, and F. Bergaya, "Surface Properties of Clay Minerals," in *Developments in Clay Science* (Elsevier B.V., 2015), 5 (Chapter 1).
128. N. Mitter, E. A. Worrall, K. E. Robinson, et al., "Clay Nanosheets for Topical Delivery of RNAi for Sustained Protection against Plant Viruses," *Nature Plants* 3 (2017): 16207.
129. A. B. Subramaniam, J. Wan, A. Gopinath, and H. A. Stone, "Semi-Permeable Vesicles Composed of Natural Clay," *Soft Matter* 7 (2011): 2600.
130. S. J. Eichhorn, "Cellulose Nanowhiskers: Promising Materials for Advanced Applications," *Soft Matter* 7 (2011): 303.
131. R. J. Moon, G. T. Schueneman, and J. Simonsen, "Overview of Cellulose Nanomaterials, their Capabilities and Applications," *JOM* 68 (2016): 2383.
132. A. Ferrer, L. Pal, and M. Hubbe, "Nanocellulose in Packaging: Advances in Barrier Layer Technologies," *Industrial Crops and Products* 95 (2017): 574.
133. T. R. Arruda, G. de O. Machado, C. S. Marques, et al., "An Overview of Starch-Based Materials for Sustainable Food Packaging: Recent Advances, Limitations, and Perspectives," *Macromol* 5 (2025): 19.
134. S. Paunonen, "Strength and Barrier Enhancements of Cellophane and Cellulose Derivative Films: A Review," *Bioresources* 8 (2013): 3098.
135. K. Syverud and P. Stenius, "Strength and Barrier Properties of MFC Films," *Cellulose* 16 (2009): 75.
136. S. Singh, G. Şahin, F. A. G. S. Silva, et al., "Development of Bio-Based Coatings Incorporating Microfibrillated Cellulose, Lignin and Ionomer Dispersions for Food Contact Applications," *Packaging Technology and Science* 38 (2025): 613.
137. C. Schütz, J. R. Bruckner, C. Honorato-Rios, Z. Tosheva, M. Anyfantakis, and J. P. F. Lagerwall, "From Equilibrium Liquid Crystal Formation and Kinetic Arrest to Photonic Bandgap Films Using Suspensions of Cellulose Nanocrystals," *Crystals (Basel)* 10 (2020): 199.
138. Y. Habibi, L. A. Lucia, and O. J. Rojas, "Cellulose Nanocrystals: Chemistry, Self-Assembly, and Applications," *Chemical Reviews* 110 (2010): 3479.
139. N. Lavoine, I. Desloges, A. Dufresne, and J. Bras, "Microfibrillated Cellulose—Its Barrier Properties and Applications in Cellulosic Materials: A Review," *Carbohydrate Polymers* 90 (2012): 735.
140. J. Wang, D. J. Gardner, N. M. Stark, D. W. Bousfield, M. Tajvidi, and Z. Cai, "Moisture and Oxygen Barrier Properties of Cellulose Nanomaterial-Based Films," *ACS Sustainable Chemistry and Engineering* 6 (2018): 49.
141. J. R. A. Pires, R. Pereira, S. Paz, et al., "Bioactive Properties of Chitosan/Nanocellulose Films Loaded with Sage Essential Oil: From In Vitro Study to In Situ Application in Shelf-Life Extension of Fresh Poultry Meat," *Journal of Composites Science* 9 (2025): 428.
142. L. Amornkitbamrung, M. C. Marnul, T. Palani, et al., "Strengthening of Paper by Treatment with a Suspension of Alkaline Nanoparticles Stabilized by Trimethylsilyl Cellulose," *Nano-Structures and Nano-Objects* 16 (2018): 363.
143. F. Delgado-Vargas, A. R. Jiménez, and O. Paredes-López, "Natural Pigments: Carotenoids, Anthocyanins, and Betalains—Characteristics, Biosynthesis, Processing, and Stability," *Critical Reviews in Food Science and Nutrition* 40 (2000): 173.
144. B. Tang, Y. He, J. Liu, et al., "Kinetic Investigation into pH-Dependent Color of Anthocyanin and Its Sensing Performance," *Dyes and Pigments* 170 (2019): 107643.
145. K. Yoshida, M. Mori, and T. Kondo, "Blue Flower Color Development by Anthocyanins: From Chemical Structure to Cell Physiology," *Natural Product Reports* 26 (2009): 884.
146. X. Zhou, X. Yu, F. Xie, et al., "PH-Responsive Double-Layer Indicator Films Based on Konjac Glucomannan/Camellia Oil and Carrageenan/Anthocyanin/Curcumin for Monitoring Meat Freshness," *Food Hydrocolloids* 118 (2021): 106695.
147. K. K. Hazarika, A. Konwar, A. Borah, A. Saikia, P. Barman, and S. Hazarika, "Cellulose Nanofiber Mediated Natural Dye Based Biodegradable Bag with Freshness Indicator for Packaging of Meat and Fish," *Carbohydrate Polymers* 300 (2023): 120241.
148. A. G. Souza, R. R. Ferreira, L. C. Paula, S. K. Mitra, and D. S. Rosa, "Starch-Based films Enriched with Nanocellulose-Stabilized Pickering Emulsions Containing different Essential Oils for Possible

- Applications in Food Packaging,” *Food Packaging and Shelf Life* 27 (2021): 100615.
149. A. Fornari, M. Rossi, D. Rocco, and L. Mattiello, “A Review of Applications of Nanocellulose to Preserve and Protect Cultural Heritage Wood, Paintings, and Historical Papers,” *Applied Sciences* 12 (2022): 12846.
150. P. Baglioni and R. Giorgi, “Soft and Hard Nanomaterials for Restoration and Conservation of Cultural Heritage,” *Soft Matter* 2 (2006): 293.
151. X. Wu, H. Mou, H. Fan, J. Yin, Y. Liu, and J. Liu, “Improving the Flexibility and Durability of Aged Paper with Bacterial Cellulose,” *Materials Today. Communications* 32 (2022): 103827.
152. C. Reynaud, M. Thoury, A. Dazzi, et al., “In-Place Molecular Preservation of Cellulose in 5,000-Year-Old Archaeological Textiles,” *Proceedings of the National Academy of Sciences* 117 (2020): 19670.
153. Y. Dong, Y. Xie, X. Ma, et al., “Multi-Functional Nanocellulose Based Nanocomposites for Biodegradable Food Packaging: Hybridization, Fabrication, Key Properties and Application,” *Carbohydrate Polymers* 321 (2023): 121325.
154. S. Y. H. Abdalkarim, L.-M. Chen, H.-Y. Yu, et al., “Versatile Nanocellulose-Based Nanohybrids: A Promising-New Class for Active Packaging Applications,” *International Journal of Biological Macromolecules* 182 (2021): 1915.
155. C. E. Udoh, J. T. Cabral, and V. Garbin, “Nanocomposite Capsules with Directional, Pulsed Nanoparticle Release,” *Science Advances* 3 (2017): eaao3353.
156. D. Mame-Khady, T. Yasui, S. Sugiyama, et al., “Edible Liquid Marbles Stabilized with Millimeter-Sized Spherical Particles,” *Current Research in Food Science* 9 (2024): 100899.
157. E. Mukai, C. Dari, T. Yasui, T. Yagishita, A. Fameau, and S. Fujii, “Cinnamon Particle-Stabilized Gas Marbles: A Novel Approach for Enhanced Stability and Versatile Applications,” *Advanced Functional Materials* 35 (2025): 2409926.
158. F. Shiralipour, Y. N. Akhtar, A. Gilmor, G. Pegorin, A. Valerio-Aguilar, and E. Hegmann, “The Role of Liquid Crystal Elastomers in Pioneering Biological Applications,” *Crystals* 14 (2024), 859.
159. Z. Zhao, H. Li, Y. Yao, et al., “Integer Topological Defects Offer a Methodology to Quantify and Classify Active Cell Monolayers,” *Nature Communications* 16 (2025): 2452.
160. H. T. Beaman and M. B. B. Monroe, “Highly Porous Gas-Blown Hydrogels for Direct Cell Encapsulation with High Cell Viability,” *Tissue Engineering Part A* 29 (2023): 308.
161. S. A. Bencherif, R. W. Sands, D. Bhatta, et al., “Injectable Preformed Scaffolds with Shape-Memory Properties,” *Proceedings of the National Academy of Sciences* 109 (2012): 19590.
162. Y.-C. Tan, K. Hettiarachchi, M. Siu, Y.-R. Pan, and A. P. Lee, “Controlled Microfluidic Encapsulation of Cells, Proteins, and Microbeads in Lipid Vesicles,” *Journal of the American Chemical Society* 128 (2006): 5656.
163. M. He, J. S. Edgar, G. D. M. Jeffries, R. M. Lorenz, J. P. Shelby, and D. T. Chiu, “Selective Encapsulation of Single Cells and Subcellular Organelles into Picoliter- and Femtoliter-Volume Droplets,” *Analytical Chemistry* 77 (2005): 1539.
164. S. Utech, R. Prodanovic, A. S. Mao, R. Ostafe, D. J. Mooney, and D. A. Weitz, “Microfluidic Generation of Monodisperse, Structurally Homogeneous Alginate Microgels for Cell Encapsulation and 3D Cell Culture,” *Advanced Healthcare Materials* 4 (2015): 1628.
165. M. Nakamura, M. Matsumoto, T. Ito, I. Hidaka, H. Tatsuta, and Y. Katsumoto, “Microfluidic Device for the High-Throughput and Selective Encapsulation of Single Target Cells,” *Lab on a Chip* 24 (2024): 2958.
166. T. Čamo, R. Kizhakidathazhath, D. Waldmann-Diederich, and J. P. Lagerwall, “Optical Crack Detection and Assessment using Cholesteric Liquid Crystal Elastomers,” *Structural Health Monitoring* 25 (2026): 536.
167. M. M. De Luna, P. Karandikar, and M. Gupta, “Interactions between Polymers and Liquids during Initiated Chemical Vapor Deposition onto Liquid Substrates,” *Molecular Systems Design and Engineering* 5 (2020): 15.
168. J. Fujiwara, F. Geyer, H. Butt, T. Hirai, Y. Nakamura, and S. Fujii, “Shape-Designable Polyhedral Liquid Marbles/Plasticines Stabilized with Polymer Plates,” *Advanced Materials Interfaces* 7 (2020): 2001573.
169. M. Anyfantakis, D. Baigl, and B. P. Binks, “Evaporation of Drops Containing Silica Nanoparticles of Varying Hydrophobicities: Exploiting Particle-Particle Interactions for Additive-Free Tunable Deposit Morphology,” *Langmuir* 33 (2017): 5025.
170. A. R. Anwar, M. Mur, G. Michailidou, D. N. Bikiaris, and M. Humar, “Microlasers Made Entirely From Edible Substances,” *Advanced Optical Materials* 13 (2025): 2500497.
171. W. A. Curtin and R. E. Miller, “Atomistic/Continuum Coupling in Computational Materials Science,” *Modelling and Simulation in Materials Science and Engineering* 11 (2003): R33.
172. T. J. White and D. J. Broer, “Programmable and Adaptive Mechanics with Liquid Crystal Polymer Networks and Elastomers,” *Nature Materials* 14 (2015): 1087.
173. J. Abraham, K. S. Vasu, C. D. Williams, et al., “Tunable Sieving of Ions Using Graphene Oxide Membranes,” *Nature Nanotechnology* 12 (2017): 546.
174. J. Kim, H. Kim, H. Kang, et al., “A Water-Soluble Label for Food Products Prevents Packaging Waste and Counterfeiting,” *Nature Food* 5 (2024): 293.
175. S. Wang and M. W. Urban, “Self-Healing Polymers,” *Nature Reviews Materials* 5 (2020): 562.
176. W. Feng, D. J. Broer, and D. Liu, “Oscillating Chiral-Nematic Fingerprints Wipe Away Dust,” *Advanced Materials* 30 (2018): 1704970.
177. K. M. Cannon, C. B. Dreyer, G. F. Sowers, et al., “Working with Lunar Surface Materials: Review and Analysis of Dust Mitigation and Regolith Conveyance Technologies,” *Acta Astronautica* 196 (2022): 259.
178. D. V. Margiotta, W. C. Peters, S. A. Straka, et al., “The Lotus coating for space exploration: a dust mitigation tool,” in *Optical System Contamination: Effects, Measurements, and Control*, ed. S.A. Straka and N. Carosso, 7794, (SPIE, 2010): 77940I.
179. D. W. Collinson, “Lunar Sourcebook—A User’s Guide to the Moon,” *Physics of the Earth and Planetary Interiors* 72 (1992): 132.
180. T. Yada, M. Abe, T. Okada, et al., “Preliminary Analysis of the Hayabusa2 Samples Returned From C-Type Asteroid Ryugu,” *Nature Astronomy* 6 (2022): 214.
181. L. Pernigoni, U. Lafont, and A. M. Grande, “Self-Healing Materials for Space Applications: Overview of Present Development and Major Limitations,” *CEAS Space Journal* 13 (2021): 341.
182. H. Zhang, X. Cheng, C. Liu, et al., “Ultraviolet-Blocking Polymers and Composites: Recent Advances and Future Perspectives,” *Journal of Materials Chemistry A* 12 (2024): 32638.
183. H. Gao and P. Liu, “High-Temperature Encapsulation Materials for Power Modules: Technology and Future Development Trends,” *IEEE Transactions on Components, Packaging and Manufacturing Technology* 12 (2022): 1867.
184. T. Mkhari, J. O. Adeyemi, and O. A. Fawole, “Recent Advances in the Fabrication of Intelligent Packaging for Food Preservation: A Review,” *Processes* 13 (2025): 539.

185. Y. Qiu, D. Zhang, M. Long, et al., "Coassembly of Hybrid Microscale Biomatter for Robust, Water-Processable, and Sustainable Bioplastics," *Science Advances* 11 (2025): 1596.
186. A. J. Christy and S. T. Phillips, "Closed-Loop Recyclable Plastics From Poly(ethyl Cyanoacrylate)," *Science Advances* 9 (2023): 1.
187. V. Kumar, A. Elfving, H. Koivula, D. Bousfield, and M. Toivakka, "Roll-to-Roll Processed Cellulose Nanofiber Coatings," *Industrial and Engineering Chemistry Research* 55 (2016): 3603.
188. G. Guggenbiller, S. Brooks, O. King, E. Constant, D. Merckle, and A. C. Weems, "3D Printing of Green and Renewable Polymeric Materials: Toward Greener Additive Manufacturing," *ACS Applied Polymer Materials* 5 (2023): 3201.
189. S. Liu, Z. Han, and X. Luo, "A Comprehensive Review on Inkjet-Printed Intelligent Food Packaging Materials: Principle, Ink Formulation, Functional Inks, and Potential Applications," *Food Frontiers* 6 (2025): 1715.
190. R. L. Truby and J. A. Lewis, "Printing Soft Matter in Three Dimensions," *Nature* 540 (2016): 371.
191. B. A. Grzybowski, C. E. Wilmer, J. Kim, K. P. Browne, and K. J. M. Bishop, "Self-Assembly: From Crystals to Cells," *Soft Matter* 5 (2009): 1110.

## Biographies



**Venkata S. R. Jampani** is a Principal Investigator at the Jožef Stefan Institute (Ljubljana, Slovenia), where he leads the Interfacial Soft Matter Laboratory. He focuses on experimental soft matter, with an emphasis on interface-driven phenomena in liquid crystals, liquid-crystal elastomers, cellulose-based systems, colloids, and soft-matter photonics. His research investigates how liquid-crystal elasticity, interfaces, and self-assembly generate distinct geometries and topological structures in soft materials. Interface-driven mechanisms are a key strategy; his group explores how these principles can be translated into functional responses, including emerging photonic platforms based on soft matter.



**Manos Anyfantakis** is a Senior Scientist at the European Space Resources Innovation Centre. He has pursued research across soft matter and interface science at leading academic institutions and a space industry startup. The common thread is the study of materials at the interface between fundamental understanding and technological application, focusing on how the properties and interactions of diverse building blocks can be harnessed to create materials with tailored response. By extending this approach to the emerging In-Situ Resource Utilisation (ISRU), he aims to develop a solid understanding of space resources and, building on this, design advanced ISRU materials, and processes.